Pergamon

Geochimica et Cosmochimica Acta, Vol. 66, No. 3, pp. 383–402, 2002

0016-7037/02 $22.00 + .00

PII S0016-7037(01)00791-8

The adsorption of gold(I) hydrosulphide complexes by iron sulphide surfaces

A. M. WIDLER and T. M. SEWARD*

Institut für Mineralogie und Petrographie, Eidgenössische Technische Hochschule, ETH Zentrum, 8092 Zürich, Switzerland

(*Received January* 9, 2001; *accepted in revised form July* 11, 2001)

Abstract—The adsorption of gold by pyrite, pyrrhotite, and mackinawite from solutions containing up to 40 mg/kg (8 μm) gold as hydrosulphidogold(I) complexes has been measured over the pH range from 2 to 10 at 25°C and at 0.10 m ionic strength (NaCl, $NaClO_4$). The pH of point of zero charge, pH_{pzc}, has been determined potentiometrically for all three iron sulphides and shown to be 2.4, 2.7, and 2.9 for pyrite, pyrrhotite, and mackinawite, respectively. In solutions containing hydrogen sulphide, the pH_{pzc} is reduced to values below 2. The surface charge for each sulphide is therefore negative over the pH range studied in the adsorption experiments. Adsorption was from 100% in acid solutions having pH $<$ 5.5 (pyrite) and pH $<$ 4 (mackinawite and pyrrhotite). At alkaline pH's (e.g., pH = 9), the pyrite surface adsorbed 30% of the gold from solution, whereas the pyrrhotite and mackinawite surfaces did not adsorb.

The main gold complex adsorbed is AuHS°, as may be deduced from the gold speciation in solution in combination with the surface charge. The adsorption of the negatively charged $Au(HS)_2^-$ onto the negatively charged sulphide surfaces is not favoured. The X-ray photoelectron spectroscopic data revealed different surface reactions for pyrite and mackinawite surfaces. While no change in redox state of adsorbent and adsorbate was observed on pyrite, a chemisorption reaction has been determined on mackinawite leading to the reduction of the gold(I) solution complex to gold(0) and to the formation of surface polysulphides. The data indicate that the adsorption of gold complexes onto iron sulphide surfaces such as that of pyrite is an important process in the "deposition" of gold from aqueous solutions over a wide range of temperatures and pressures.

1. INTRODUCTION

Gold occurs in pyrite in hydrothermal environments throughout the Earth's crust at conditions ranging from high-grade metamorphism and near magmatic to the lower temperature regimes of epithermal ore deposition and seafloor hydrothermal systems. The precipitation of gold in hydrothermal systems is generally regarded as being determined by decreases in the equilibrium solubility due to changing gold complex stability in response to processes such as boiling and fluid mixing and associated changes in pH and reduced sulphur activity. However, the role of surface adsorption by sulphide minerals such as pyrite is seldom considered despite the demonstrated role of sulphide mineral surfaces in scavenging gold as reported by Renders and Seward (1989b), Schoonen et al. (1992), and Widler and Seward (1996, 1998). Several other recent experimental studies by Arakaki and Morse (1993), Morse and Arakaki (1993), and Kornicker and Morse (1991) have also considered the adsorption of heavy metals such as manganese by pyrite and mackinawite as a function of pH, but the nature of the adsorbed manganese on the sulphide surface was not discussed. A fundamental aspect of surface adsorption is that a trace component such as gold may be coprecipitated from a hydrothermal fluid by a phase such as pyrite at concentrations below the equilibrium saturation.

There is some evidence for the role of surface adsorption in the precipitation or concentration of gold by surface effects in ore-depositing hydrothermal systems. In a recent study, Simon et al. (1999b) suggested that 50% of the total gold in the Twin Creeks deposit, a Carlin-type deposit in the United States, had been extracted from solution during the ore-forming process by adsorption. Gold in such samples has been observed either as small inclusions of metallic gold or as submicroscopic inclusions of gold(I), which is generally termed "invisible gold" (Sha, 1993; Simon et al., 1999a, 1999b). Both have attributed the observation of at least the Au(I) to surface adsorption processes, in analogy to the studies of Renders and Seward (1989b) and Cardile et al. (1993). The similar, still active Ladolam epithermal deposit on Lihir Island contains gold reserves of 600 t and is still boiling at depth (Moyle et al., 1990). The main ore phases in the deposit are gold-enriched pyrite and native gold. In the fore-arc basin of Lihir on top of the Conical seamount volcano at a depth of 1050 m, iron sulphides containing up to 43 ppm Au have been discovered (Herzig and Hannington, 1995). In contrast to the known subaerial systems, greigite (Fe_3S_4) and amorphous FeS have been recognised in the exhalative precipitates, in addition to pyrite and marcasite.

Hydrothermal black smoker systems are favourable places for metal adsorption because of the rapid formation of large amounts of fine-grained to colloidal-sized sulphides with large specific surface areas as a consequence of cold seawater mixing with hydrothermal solutions at temperatures up to 400°C. The association of gold from such environments has been studied by Hannington et al. (1986), Hannington and Scott (1989), Hannington et al. (1991), and Herzig et al. (1993), but the fine-grained nature of the samples has inherent analytical limitations, as gold analysis of single phases is not feasible because of the low concentrations and small grain size. The chimney precipitates can be organised in three associations: (1) the high-temperature chalcopyrite-pyrrhotite-isocubanite association with low gold concentrations formed above 350°C; (2) the

* Author to whom correspondence should be addressed (tseward@erdw.ethz.ch).

medium-temperature association with pyrite and chalcopyrite with up to 4.9 ppm Au; and (3) the low-temperature phases such as sphalerite, galena, tennantite, Pb-Ag-sulfosalts, pyrite, and bornite, which can contain small inclusions of native gold (Herzig et al., 1993) and total assemblage gold concentrations of up to 30 ppm. The detailed gold contents of iron sulphide precipitates are not known and many present-day minerals may as well be the result of recrystallisation.

Experiments by Schoonen and Barnes (1991a, 1991b, 1991c, 1991d) have shown that by reacting sulphide/polysulphide solutions with iron-containing solutions at temperatures up to 150°C, an amorphous to partly crystalline FeS phase is initially formed, which reacts with the residual sulphur from the solution to form iron sulphide phases such as greigite and finally pyrite. The detailed reaction path depends on the availability of zero-valent sulphur and free oxygen as well as on the pH (Berner, 1964, 1967; Rickard, 1969, 1975, 1989, 1997; Sweeney and Kaplan, 1973; Morse et al., 1987; Luther, 1991; Schoonen and Barnes, 1991a, 1991b, 1991c, 1991d; Lennie and Vaughan, 1992, 1996; Rickard and Luther, 1997). These metastable iron sulphides (e.g., FeS) are sensitive to oxidation and are often not observed (overlooked) in epithermal ore-depositing environments. In contact with air and humidity they are fully oxidised within minutes.

Experimental studies on gold(I) complexes in solutions have demonstrated that hydrosulphide (HS^-) ligands play a fundamental role in gold transport by hydrothermal fluids in the Earth's crust. They are up to 20 orders of magnitude more stable than the equivalent chloride complexes (Seward, 1991). In active, ore-depositing geothermal systems such as Ohaaki-Broadlands, the aqueous gold chemistry and gold precipitation reactions are entirely dominated by the stability of gold(I) hydrosulphide complexes. Seward (1973), Renders and Seward (1989a), Shenberger and Barnes (1989), Vlassopoulos and Wood (1990), Pan and Wood (1994), Wood et al. (1994), Benning and Seward (1995, 1996), and Seward and Barnes (1997) have studied and summarised the aqueous chemistry of gold in more detail.

Traditionally, only solubility controls have been invoked to predict the gold concentration in hydrothermal solutions in response to changes in temperature, pressure, hydrogen fugacity, pH, and ligand concentration. The scavenging of gold by mineral sulphide surfaces, by means of adsorption, surface precipitation, and surface reduction, has been largely ignored. In recent years, more interest has been given to the metal adsorption on sulphides. Studies by Bancroft and Jean (1982), Jean and Bancroft (1985, 1986), Bancroft et al. (1988), Hyland and Bancroft (1989), Bancroft and Hyland (1990), Eggleston and Hochella (1993), Mycroft et al. (1995a), Scaini et al. (1995, 1997, 1998), Maddox et al. (1996, 1998), and Becker et al. (1997) have investigated the adsorption of various heavy metals onto sulphides (arsenopyrite, pyrite, pyrrhotite, marcasite, sphalerite, cinnabar, galena, molybdenite, and pentlandite) using X-ray photoelectron spectroscopy (XPS), scanning electron microscopy (SEM), secondary ion mass spectroscopy (SIMS), Auger spectroscopy, and Rutherford backscattering spectroscopy. Studies of gold adsorption onto pyrite by Jean and Bancroft (1985) (Au[III] chlorides), Mycroft et al. (1995a) (Au[I] and Au[III] chlorides), and Maddox et al. (1998) (Au[III] chlorides) observed (using XPS) a two-step reaction forming first a metastable Au(I) surface complex, which further reacted to metallic gold. Schoonen et al. (1992) and Mirnov et al. (1981) have studied the interaction of very low gold concentrations in water and chloride solutions at variable pH with pyrite. Only the study of Scaini et al. (1998), in which Au(I) hydrosulphide complexes were present in solution, showed that at least some adsorbed gold was retained on pyrite surfaces in the Au(I) state, although Au(0) was also present. In general the oxidation of surface sulphur was observed. Because of the long reaction times of their experiments, contamination by atmospheric oxygen and light may have affected their results.

Table 1. Summary of electrophoresis studies of unoxidised iron sulphides and sulphur.

Mineral	Isoelectric point	Source
Pyrite (natural)	2	Ney (1973)
Pyrite (natural)	1.2 (±0.4)	Fornasiero et al. (1991)
Pyrite (natural)	1.x to 2.3	Bebié et al. (1998)
Greigite (synthetic)	3.0 to 3.5	Dekkers and Schoonen (1994)
Pyrrhotite (natural)	2	Ney (1973)
Pyrrhotite (synthetic)	2.0 to 2.5	Dekkers and Schoonen (1994)
Pyrrhotite (natural)	2.3 to 3.5	Bebié et al. (1998)
Sulphur (synthetic)	<2.6 to 3.1[a]	Schoonen and Barnes (1988)
Sulphur (synthetic)	<3	Chander et al. (1975)
Sulphur (synthetic)	2.2	Kelebek and Smith (1989)

[a] Estimated from flocculation rates.

In addition to the above-mentioned studies involving iron sulphide surfaces, the adsorption of gold(I) hydrosulphide complexes onto amorphous arsenic and antimony sulphide has been studied by Renders and Seward (1989b), and this formed the experimental foundation for the present study. They observed gold adsorption at acid pH by both phases. With Mössbauer spectroscopy (Seward and Cardile, 1991; Cardile et al., 1993), they demonstrated the existence of a single oxidation state in form of a linear, triatomic Au(I) surface complex. The adsorption of gold(I) hydrosulphide complexes by iron sulphide surfaces has also been previously reported by Widler and Seward (1996, 1998).

The variation of the surface charge also plays an important role in metal adsorption by sulphide mineral surfaces. A few early electrophoresis studies (e.g., Ney, 1973) reported a pH_{pzc} for pyrite of ≈7 because of oxidation of the surface being studied. More recent electrophoretic measurements by Fornasiero et al. (1992), Dekkers and Schoonen (1994), and Bebié et al. (1998) suggest a $pH_{pzc} \approx 2$ for pyrite. The literature data are summarised in Table 1.

Surface reactivity and composition of iron sulphides is of much interest in several other fields; these include the early history of life (Wächtershäuser, 1988, 1990; Drobner et al., 1990; Russell et al., 1994; Russell and Hall, 1997; Cody et al., 2000), mineral flotation (Ney, 1973; Healy and Moignard, 1976; Buckley and Woods, 1984, 1985a, 1985b, 1987, 1995, 1997; Buckley et al. 1984; Kelebek and Smith, 1989; Buckley and Riley, 1991; Sun et al., 1991; Pratt et al., 1994; Nesbitt et al., 1995, 1998; Vaughan et al., 1997; Schaufuss et al., 1998a), and photovoltaic effects of pyrite (Dasbach et al., 1993; Bronold et al. 1994a, 1994b).

The scope of this study is the evaluation of gold(I) hydrosulphide adsorption by the different iron sulphides as a function

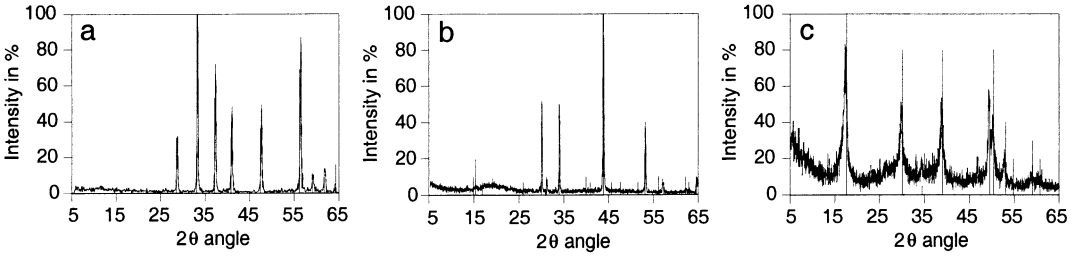

Fig. 1. X-ray diffractograms of synthetic mineral phases: (a) pyrite, (b) pyrrhotite, and (c) mackinawite measured with Cu K_α radiation.

of pH. The primary aim of this research has therefore been to address the frequently encountered association of gold with pyrite from a surface chemistry point of view. This has involved a multipronged approach, including (1) the synthesis of the three iron sulphides (pyrite, pyrrhotite, and mackinawite), (2) the determination of their surface charge properties (i.e., pH_{pzc}) by potentiometric titration, (3) the adsorption of gold(I) hydrosulphide complexes on these sulphide surfaces as a function of pH, and (4) the application of XPS to gain insight into the nature of adsorbed gold on surfaces of pyrite and mackinawite.

Careful synthesis of the various iron sulphides provided crystalline material with pristine surfaces that were not contaminated by atmospheric oxygen and "undamaged," as would be the case with crushed, natural mineral grains. This material was then used in the potentiometric titrations of surface charge to determine the pH_{pzc}. A knowledge of the charge of iron sulphide mineral surfaces is important to the understanding of the adsorption mechanism, bearing in mind that negatively charged species are not easily adsorbed onto negatively charged surfaces. The reason for studying mackinawite adsorption was because iron monosulphide is considered to be an important precursor in pyrite formation at $t < 200$°C (see, e.g., Schoonen and Barnes, 1991a, 1991b, 1991c, 1991d) and the adsorption behaviour could be important in understanding the nature of the observed concentration in some natural pyrites. Finally, the gold adsorbed onto pyrite and mackinawite was studied using XPS to establish whether gold(I) surface complexes were present or if chemisorptive redox reactions had occurred, leading to the formation of Au(0).

2. EXPERIMENTAL METHODS

2.1. Mineral Synthesis

The adsorption of gold(I) hydrosulphide complexes has been measured on pyrite, pyrrhotite, and mackinawite surfaces using both synthetic and natural phases. For the adsorption experiments, monophase, crystalline samples with pristine, unoxidised surfaces are required. Ideally, such samples should have a homogeneous particle size so that adsorbent and adsorbate can be separated by filtration. The general strategy for the synthesis was to react a sulphur-containing solution with an iron-containing solution at a given temperature, pressure, and pH over a range of temperatures from 25 to 240°C and pressures up to 100 bar.

Sulphide mineral syntheses up to 90°C were conducted in 1-L glass vessels having a number of ports, which permitted the continuous monitoring of pH (Ross electrode) as well as the addition and removal of reactants and products under an atmosphere of oxygen-free nitrogen. The deoxygenated nitrogen employed in these experiments was produced by passing commercially available "oxygen-free nitrogen" through a 50-cm-long column of copper filings maintained at 420°C. The hydrothermal synthesis experiments were conducted in a stainless steel autoclave of 100 ml volume that was mounted vertically in a simple resistance furnace, the temperature of which was controlled and monitored to ±2°C. Pressure was controlled and monitored by a back-pressure regulator and a pressure gauge that were connected to the reaction autoclave via a stainless steel separator vessel containing a mobile piston. Solution could also be added to and reacted with hot solution in the reaction vessel by injection under pressure using a spindle press.

The surface area was determined by BET nitrogen adsorption (10-point measurement) using a Micromeritics Gemini 2360 apparatus with gas quality grades of 5.0 (99.999%) for nitrogen and helium. The mineral suspension was initially filtered under nitrogen and the precipitate transferred to tubes and dried. In the case of pyrite and pyrrhotite, the precipitate was dried for 2 h at 200°C in vacuum. The mackinawite sample was not heated but dried in vacuum for 12 h to avoid recrystallisation.

The synthesis of pyrite proved to be rather troublesome, mainly because of our requirements that the synthesised product must be monomineralic and thus free of other phases. The methods described by Berner (1964), Rickard (1969, 1997), and Schoonen and Barnes (1991a, 1991b, 1991c, 1991d) produced pyrite that was usually associated with varying amounts of other iron sulphide phases. This was unacceptable because the presence of additional phases would mean that the adsorption of gold from solution could also be affected by mineral phases other than pyrite.

In this study, pyrite was synthesised using a method similar to that described by Wei and Osseo-Asare (1995). Two solutions (0.067 m NaHS and 0.034 m $FeCl_3$) were prepared using deoxygenated water and mixed in a glass reaction vessel at 80°C. The pH was adjusted to pH ~ 3.5 and the mixture allowed to react for 36 h. As a precaution, the filtered product was then washed with 1 m HCl to remove any iron sulphide phases other than pyrite. X-ray diffraction measurements confirmed that the resulting pyrite was well crystallised and no other phases could be detected (Fig. 1a). Given the sensitivity of the X-ray diffractometer, contaminant phases might have been present at a <1 to 2% level. Nevertheless, fine-grained amorphous FeS and other sulphide minerals would have been removed during the acid washing procedure.

Natural pyrite (Huanzala, Peru) was also employed in some of the adsorption experiments and potentiometric titrations. This material was crushed and sieved and the <125-μm fraction subsequently washed in 6 N HCl, deoxygenated ethanol and dried under vacuum. This material had a BET surface area of 4.5 m^2/g.

Pyrrhotite was synthesised hydrothermally. A 0.30-m NaHS solution containing 0.05 m KH_2PO_4 and 0.01 m Na_2HPO_4 was heated to 230°C and 100 bar. A solution of 1.10 m Mohr's salt ($FeSO^4 \cdot (NH_4)_2SO_4$ $6H_2O$) was then injected into the autoclave using a spindle press and the system allowed to react for 10 h. The resulting product was monomineralic, well crystalline (Fig. 1b), and had a BET surface area of 16.8 m^2/g.

Mackinawite was synthesised by reaction of H_2S/HS^- solutions with Fe^{2+} in a deoxygenated environment over a range of temperatures from 25 to 130°C. The preferred method involved preheating a 0.30-m NaHS solution containing phosphate buffer (i.e., 0.05 m KH_2PO_4/0.01 m

Na_2HPO_4) to 130°C at 100 bar. A 1.10 m solution of Mohr's salt was then injected into the hot reaction vessel and allowed to react for 20 h. This produced a crystalline mackinawite (Fig. 1c) with a BET surface area of 80 m^2/g.

2.2. Potentiometric Titrations

Potentiometric titration permits the determination of the pH_{pzc} and can provide additional information about the number of the reactive surface sites. A mineral suspension is titrated against acids and bases and the pH as a function of titre is recorded. The stoichiometric point, as observed with acids and bases, represents the pH_{pzc}. From the difference of titre needed to reach a certain pH between sample suspension and blank solution and knowing the amount of solid added and its specific surface area, the density of reactive surface sites can be calculated.

The surface charges of both natural and synthetic pyrite, synthetic pyrrhotite, and synthetic mackinawite were determined by potentiometric titration at 25°C. The titre solutions were prepared with deoxygenated water and stored in flasks under an oxygen-free nitrogen atmosphere. Fresh solutions were prepared after 2 d. The acid titre was standardised by titration against a solution prepared from recrystallised borax. NaOH titre was standardised against the acid titre. About 1.35 m^2 of sulphide mineral surface area was titrated in each experiment.

For the titrations, a potentiostat/titrator (Metrohm GP736 Titrino) with an additional external plunger pump (Dosimat 685), both with 20 mL volume, were used. The measured values of pH were stable to within 2 mV/min (equivalent of pH change of 0.033 pH unit/min or a minimal waiting time of 26 s before further addition of 0.05 ml of titre). The pH was monitored with an Orion Ross 8102 combination electrode and recorded by the Metrohm TiNet software package for further evaluation and processing. The inlet ports of the reaction vessels were sealed by Viton/silicon/Teflon rings. During the experiments, the vessel was kept under a small nitrogen overpressure to avoid ingress of air. The solid was added as a suspension after the determination of its surface area. In the titrations, the suspensions were first titrated down to pH = 1.2 by addition of $HCl/HClO_4$ and afterward by addition of NaOH until pH = 12 was reached. The titration curves for both titration directions were recorded, but only the titration with acid showed a reaction with the surface.

2.3. Gold Adsorption

The adsorption of aqueous gold(I) hydrosulphide complexes by natural and synthetic pyrite, synthetic pyrrhotite, and synthetic mackinawite was studied over the pH range from 2 to 10 at 25°C and ionic strength equal to 0.1 m NaCl. The concentration of gold in solution was always below equilibrium saturation, and the ratio of sulphide mineral surface area to total gold in solution was maintained constant. Gold(I) hydrosulphide stock solutions were prepared by the reaction of fine-grained elemental gold and a sulphide solution containing 0.15 m total reduced sulphur at pH $\approx$ 7 at 20°C.

The aqueous sulphide solutions were prepared by bubbling H_2S through a 0.075-m NaOH solution made from deoxygenated water until pH $\approx$ 7 was obtained. The equilibration of the near-neutral sulphide solution with the fine-grained gold precipitate was carried out at 20°C in a glass flask wrapped in aluminium foil that was stirred continuously and kept in the dark. After 5 d, a solution containing $\sim$10 mg/kg of gold was obtained. The concentration was determined by inductively coupled plasma mass spectroscopy (ICP-MS).

The adsorption experiments were carried out in stirred, black glass reaction vessels of 0.5 and 2.0 l volume that were immersed in a thermostated water bath at 25°C. Initially, aliquots of mineral suspension and sodium chloride or sodium perchlorate were added to a given volume of saturated (1 bar at 25°C) H_2S solution in the reaction vessel. A titrator/potentiostat (Metrohm Titrino 736) and a Ross combination pH electrode were used to monitor the pH, which was adjusted by addition of HCl, $HClO_4$, or NaOH to the required pH. A suitable aliquot of gold(I) hydrosulphide stock solution was then added and the pH further adjusted as required.

At this point, a number of aspects should be further emphasised. Firstly, all aspects of the solution and sample preparation must be free from reactive oxygen (air) contamination. Not only must the mineral surfaces be uncontaminated by oxidation but the solutions as well, as the acid and base titre must be deoxygenated and handled under deoxygenated nitrogen. Secondly, the preparation of gold-containing solutions as well as the adsorption experiments themselves must be free of light contamination to avoid the photoreduction of light sensitive Au(I) species to Au°. And thirdly, care must be taken when adding the gold stock solution to the sulphide solution in the adsorption reaction vessel that the solution remains undersaturated when the pH is adjusted to acid or alkaline conditions, in order to avoid the precipitation of Au_2S. This may be monitored by calculation of the solubility of Au_2S at various pHs and total reduced sulphur concentrations using the thermodynamic data of Renders and Seward (1989a) and Suleimenov and Seward (1997).

Experiments with high gold concentration and long reaction times up to 10 h (initial gold concentration $\approx$ 350 μg/kg, solution volume = 1.6 l, mineral surface area per experiment $\approx$ 4.5 m^2) were performed with synthetic pyrite. Experiments with lower gold concentration (initial gold concentration $\approx$ 40 μg/kg, solution volume = 0.42 l, mineral surface area per experiment $\approx$ 2 m^2) were performed with natural, acid-cleaned pyrite, synthetic pyrrhotite, and synthetic mackinawite. The iron sulphide phases onto which gold had been adsorbed were filtered, dried, and weighed. The samples were digested in aqua regia contained within a Teflon reaction vessel in a microwave oven. The total iron was then determined using an Iris ICP optical emission spectroscopy facility with an analytical precision of $\pm$3%.

Gold analyses were performed using a Perkin Elmer ELAN 6000 ICP mass spectroscope. Thallium was used as internal standard, and indium, cobalt, and cerium were additionally measured to provide further information about sample and system stability. For the sample preparation, only "Suprapur" reagents (Merck: HCl 30%, HNO_3 65%, H_2O_2 30%) and doubly distilled (in quartz glass), deionised water were used. Liquid samples from the adsorption experiments were transferred to flat bottomed flasks, acidified with HCl under nitrogen stream to allow H_2S to escape and evaporated to near dryness. Four ml of aqua regia were added, and the solution was brought up to boiling, cooled, and diluted to 10 ml. Then, 0.2 ml of a 799 μg/kg Tl standard was added.

2.4. XPS Measurements

XPS is a surface-sensitive technique that provides a semiquantitative analysis of chemical composition as well as giving insight into the oxidation and binding state of the elements involved. X-rays with energy $E_{X\text{-}ray}$ are used to eject core electrons from surface atoms. By measuring their kinetic energy, E_{kin}, the binding energy, E_{bin}, of the core electrons can be determined, defined as

$$E_{bin} = E_{X\text{-}ray} - E_{kin}. \quad (1)$$

The binding energy of the core electrons depends on the oxidation state and on the binding partners of the elements. For example, the binding energy of the sulphur $2p_{3/2}$ electrons for sulphide (S^{2-}) is approximately 162 eV, whereas for elemental sulphur, the binding energy is $\sim$164.2 eV and is 169.0 eV for sulphate (SO_4^{2-}). In general, the more oxidised an element, the higher the core electron binding energy.

However, the detection limits for conventional XPS mean that higher gold concentrations are required on the sulphide mineral surfaces to obtain useful spectra. This was accomplished by decreasing the mass of solid onto which gold was adsorbed while increasing the total amount of gold available for adsorption by adding larger volume of gold-containing stock solution to the system. Gold was adsorbed onto 0.02 g of pyrite and mackinawite at pH = 4 during a 3 h run time to give a maximum calculated loading of 39 g/kg Au in pyrite and mackinawite. The "gold-adsorbed" suspensions were then filtered under oxygen-free nitrogen and dried in a desiccator over silica gel under the same atmosphere. The samples (i.e., gold-containing iron sulphide on cellulose nitrate membrane filters) were mounted onto the XPS sample plate under a stream of nitrogen to minimise contact with atmospheric oxygen.

X-ray photoelectron spectra were obtained on a Specs Sage 100 system operating at a base back pressure of less than 7×10^{-8} bar. The X-ray source was focused on a study area of 3 $\times$ 4 mm. Overview and

narrow-region XPS scans were recorded at an analyser pass energy of 50 and 14 eV respectively, using a hemisphere detector and Mg K_α X-rays (12 kV and 25 mA) as exciting radiation. With the Mg K_α radiation employed (conventional X-ray tube, no monochromator), a sample depth of ~50 Å was studied. The spectrum measured for metallic gold foil gave a full width at half maximum (FWHM) of 1.05 eV with 85% Lorentzian and 15% Gaussian contributions to the peak shape.

With nonmetallic mineral powders, the correction of the shift originating from the charging of the sample presents a major problem. In most cases, the static charge effect, which occurs with nonmetals, is corrected by setting the carbon 1s electron binding energy to 284.6 eV (the carbon originates from oil within the apparatus). In our samples, the carbon is from residual polydimethlysilicone (PDMS), a major compound of silicon vacuum grease. For PDMS, the following binding energies are tabulated (Beamson and Briggs, 1992): C 1s 284.38 eV, O 1s 532.0 eV, and Si $2p_{3/2}$ 101.79 eV relative to O 1s to 532.0 eV. To decide which binding energy of C 1s to use to correct the spectrum for surface charge, the S $2p_{3/2}$ values of pyrite were employed. Setting the C 1s electron binding energy to 284.6 eV, the resulting electron binding energy was within the range of binding energies determined in other studies (see "Results") on pyrite and was therefore preferred.

Background subtraction was performed using the algorithm proposed by Shirley (1972). Au 4f, C 1s, O 1s, S 2p, and Si 2s electron binding energy spectra were fitted after background correction with symmetric curves of mixed Gaussian and Lorentzian character, including the Mg $K_{\alpha 3,4}$ satellites. The fitting of the Fe 2p spectra were performed with the additional inclusion of asymmetry terms, which account for the asymmetry caused by the many-body effect, as mentioned under "Results." For the iterative fitting procedure, the robust algorithm in the pro Fit software package (*Pro Fit 5.1 User's Manual*, 1998) was applied using the equations from Briggs and Rivière (1983) for the peak shape.

3. RESULTS

3.1. Potentiometric Titrations and Surface Charge

Potentiometric titration methods have been extensively employed in determining the pH_{pzc} of oxides (Parks and De Bruyn, 1962; Stumm and Morgan, 1981; Sposito, 1984; Dzombak and Morel, 1990), but studies of sulphide surfaces are rare. Potentiometrically derived pH_{pzc} data exist for sphalerite, galena (Sun et al., 1991), arsenic and antimony sulphide (Renders and Seward, 1989b). Other studies on the charge development of sulphides have employed electrophoresis or flocculation methods to study the surface charge as a function of pH. Most are aimed at increasing mineral separation efficiency in flotation processes with additives such as cyanide or organic ligands (i.e., xanthate). Little interest has been focused on the nature of the surface sites or the details of the surface reactions.

The sensitivity of sulphide surfaces to oxidation is well illustrated by the various electrophoresis studies of sphalerite and pyrite. For sphalerite, isoelectric points, the equivalent to pH_{pzc} (potentiometric titration), of below pH 2 and up to pH 8 have been measured (Bebié et al., 1998; Healy and Moignard, 1976; Ney, 1973; Williams and Labib, 1985). For pyrite, the pH interval varies from 1.2 to 7 (Bebié et al. 1998; Fornasiero et al., 1992; Healy and Moignard, 1976; Ney, 1973). The low pH values are interpreted to represent the fresh, unoxidised surfaces, and the high pH determinations represent oxidised surfaces.

In the standard method, a suspension of iron sulphide in aqueous solution with a given ionic strength (0.001 to 1 m) is titrated with acid or base of the same ionic strength over the pH range to be studied. Blank titrations are also performed without the solid phase, and these curves are then subtracted from the titrations containing solid. In an ideal perfect plot, all these lines intersect at one point, which represents the pH_{pzc}, as shown, for example, by Parks and De Bruyn (1962). This technique has been developed and extensively used in the study of oxides. Potentiometric titration of oxide surfaces may generally be performed in systems open to air and hence are quite straightforward.

However, the titration of metal sulphide surfaces is very much more difficult, as will be detailed below. The solid surface must be completely uncontaminated by reaction with atmospheric oxygen, and in addition, the aqueous suspension must be free of atmospheric oxygen, as must all reagents employed. Fresh, unoxidised sulphide surfaces have a pH_{pzc} at low pH, generally between 1 and 4. To be able to reach such low pHs without adding large volumes of titre, relatively concentrated acids have to be used. If, for example, 0.10 m acid is used, the ionic strength is fixed at an inconveniently high value, and order of magnitude variations in the ionic strength are also not feasible.

Some sulphides, such as pyrrhotite and mackinawite, are known to possess an increased solubility at low pH as indicated by the solubility product for the three sulphides studied in this research (see, e.g., Davidson, 1991). The high solubility and often rapid dissolution rates for a phase such as mackinawite make an accurate determination of the pH_{pzc} almost impossible.

Finally, it should be mentioned that all standard electrolyte salts such as NaCl, $NaClO_4$, and $NaNO_3$ and their equivalent acids are potentially problematic in the titrations of sulphide surfaces. For example, the formation of Fe^{2+} chloride complexes (Heinrich and Seward, 1990) may enhance iron sulphide mineral dissolution because of iron(II) chloride complexing. In addition, perchlorate and nitrate may act as oxidising agents in higher concentrations.

Given the limitations and difficulties noted above, the approach taken in evaluating the pH_{pzc} was as follows. The uncorrected (for blank) titration data for various ionic strengths together with blank data (without solids and salts) were plotted against pH. The set for pyrrhotite is shown in Figure 2a. Only the curve with no added salt shows a change in shape. Figure 2b shows this behaviour in detail for pyrrhotite in comparison to the blank. An inflection is observed, which offsets the low-pH part of the titration curve to higher values between pH = 2.3 and 2.9 as the surface becomes protonated. The pH_{pzc} is defined as the pH at which there are as many positively charged as negatively charged surface groups such that the total charge is zero. If only one inflection is observed, which represents the reaction with only one kind of active surface site, then the pH_{pzc} is at the half height of the inflection, where half of the sites are occupied. The position of the half height of the inflection is marked with a vertical line in the graphs (Figs. 2 to 4). For pyrrhotite, this is at about pH = 2.7. Similar data are shown for mackinawite in Figure 3 , where the pH_{pzc} is estimated to be 2.9.

The pH_{pzc} is defined as the pH at which the net charge on the surface is zero. In the case of synthetic pyrite, different explanations for the two inflections (Fig. 4a) are possible. One includes a site-specific sensitivity where the two sites are protonated at different pHs. The other case includes the further protonation of a surface site that was already partially proton-

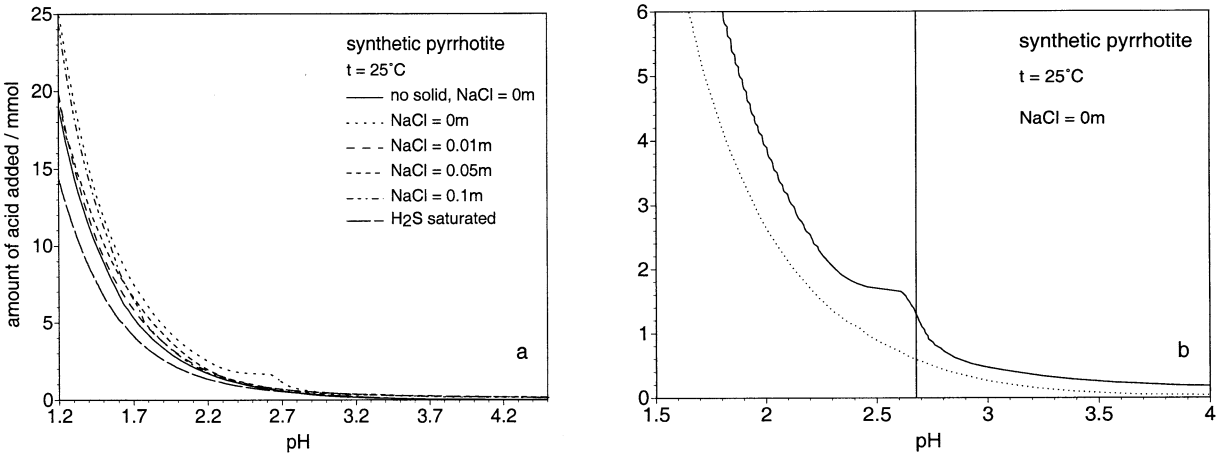

Fig. 2. Potentiometric titration results for pyrrhotite suspensions at 25°C with the initial starting volume = 141 ml (a) at various initial salt concentrations and for blank sample without added salt and (b) for pyrrhotite suspension (solid line) and blank sample (dotted line) without added salt. Vertical line marks position of pH of point of zero charge.

ated in an earlier step. Photoemission of adsorbed xenon studies by Guevremont et al. (1997, 1998) suggest the presence of at least two types of sites on the (100) surface of pyrite, one of which is associated with the normal stoichiometric surface and the other being an anion vacancy or sulphur-deficient defect site. The lower pH inflection is considered to represent the pH_{pzc} at which all negative charges have been neutralised.

The different behaviour of synthetic (Fig. 4a) and natural (Fig. 4b) pyrite cleaned with diluted HCl is to be expected because in the process of fracturing pyrite crystals, Fe^{2+}-S^{2-} and S^{2-}-S^0 bonds are broken. Surface sites therefore exist (i.e., $=Fe^{2+}$, $=S^-$ and $=S\text{-}S^{2-}$) with different charges depending on bond saturation because of different structural positions (i.e., in a plane, on the corner, or at the edge). Spectroscopic studies by Schaufuss et al. (1998a, 1998b) and Nesbitt et al. (1998) using synchrotron and conventional XPS have observed this

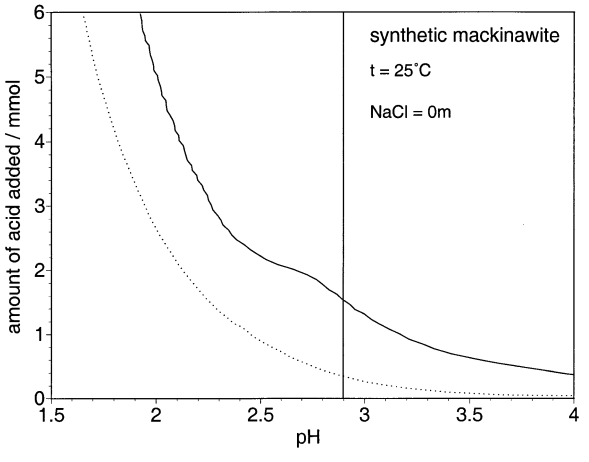

Fig. 3. Potentiometric titration results for mackinawite suspension (solid line) and blank sample (dotted line) without any salt added at 25°C with the initial starting volume = 282 ml. Vertical line marks position of pH of point of zero charge.

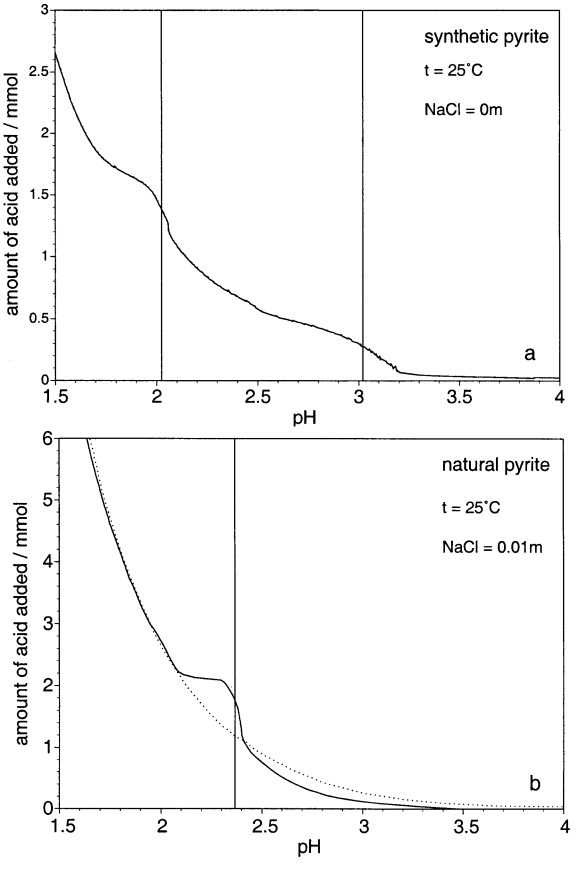

Fig. 4. Potentiometric titration results at 25°C (a) for synthetic pyrite suspension without any salt added, initial starting volume = 32 ml, vertical lines mark positions half height of the inflections; and (b) for natural pyrite suspension (solid line) with 0.01 m initial NaCl concentration and blank sample (dotted line) without any salt added, initial starting volume = 141 ml, vertical line marks position of pH of point of zero charge.

Table 2. Potentiometrically determined points of zero charge (pH_{pzc}) for iron sulphides in this study.

Mineral	Point of zero charge
Pyrite (synthetic)	2.0
Pyrite (natural)	2.4
Pyrrhotite (synthetic)	2.7
Mackinawite (synthetic)	2.9

effect. Their studies showed the high reactivity of the singly charged S^- atom, which reacts with surface Fe^{2+} sites to form Fe^{3+} and S^{2-}. The synthetic pyrite has been formed without this fracturing, and therefore, not all the same surface sites exist.

All potentiometric titrations of iron sulphide suspensions exhibited a response from the surface only at low ionic strength. For pyrrhotite and mackinawite, the titrated suspensions were free of background electrolyte. For natural pyrite, it was possible to observe an inflection at a background electrolyte concentration of 0.01 m. All suspensions saturated with hydrogen sulphide showed no surface response. Similar observations have been made by Bebié et al. (1998), who showed that pyrite acquired a negative surface charge over the entire measured pH range down to pH = 2 in solutions containing appreciable concentrations of H_2S or HS^-. Thus, H_2S and HS^- are apparently potential determining species for the iron sulphide surfaces. The potentiometrically determined pH_{pzc} data for pyrite, pyrrhotite, and mackinawite obtained in this study are summarised in Table 2 and are in good agreement with the values determined by electrophoresis (Table 1).

3.2. Adsorption Experiments

The adsorption of gold(I) hydrosulphide complexes onto iron sulphide mineral surfaces has been measured at 25°C over the pH range from 2 to 10 and 0.1 m ionic strength. The time taken to obtain equilibrium adsorption by the different sulphide surfaces was normally about 1 h at intermediate pH, and in the low pH experiments, equilibrium is achieved within 20 min. Experiments with high gold concentrations using synthetic pyrite phases did not reach equilibrium after 6 h, which may possibly be attributed to contamination by reactive oxygen (air) and/or the influence of light (photoreduction of gold[I]). Therefore, for the more sensitive monosulphides, the maximum reaction time was never more than 45 min. At low pH, only a few minutes were necessary to reach equilibrium.

All results of the adsorption experiments are presented in terms of percentage gold adsorbed and remaining in solution vs. time plots for each pH and mineral and summarised in Figures 5 to 7. Some of the experiments show some scatter in the data. This may arise from such factors as the sensitivity of the experiments to possible photoreduction of the Au^+ to metallic gold by light, the surface oxidation by oxygen contamination and sensitive sampling procedure, as well as to analytical precision because of the gold concentrations used in the experiments.

For both the natural and synthetic pyrite, maximum adsorption was observed at pH $\leq$ 5 (Fig. 5). At higher pH, the percentage gold adsorbed from solution decreased but did not fall below ~30% at pHs up to 10 (Fig. 5). Thus, adsorption extends to higher pH than with either of the two monosulphides. The comparison of both natural and synthetic pyrite with different gold concentrations shows equivalent behaviour within the experimental error. A maximum surface loading of 0.057 and 0.26 atoms/nm^2 for natural and synthetic pyrite, respectively, resulted in concentrations of 91 mg/kg for natural and 340 mg/kg for synthetic pyrite.

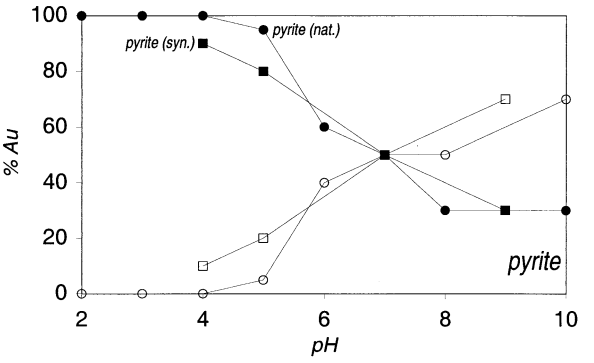

Fig. 5. Adsorption of gold(I) hydrosulphide complexes by pyrite (squares: synthetic; circles: natural) at 25°C. Percentage of total gold in solution (open symbols) and adsorbed (filled symbols) on pyrite as a function of pH. For details, see "Experimental Methods."

Pyrrhotite and mackinawite show similar adsorption behaviour (Figs. 6 and 7). The adsorption is complete at pH = 2 and decreases until pH $\geq$ 6, at which the adsorption is zero within the limits of analytical error. For pyrrhotite, a maximum surface loading of 0.086 atoms of gold per nm^2, equivalent to 470 mg/kg, is measured.

In the case of mackinawite, the attainment of equilibrium gold adsorption takes place within 25 min, with a maximum adsorption of 80% observed at pH = 3 (Fig. 7). However, at pH = 2.5, a lower adsorption (25%) was obtained, which is regarded as the effect of rapid mineral dissolution caused by increased solubility. At pH > 3, the adsorption rapidly decreases. Based on the known specific surface area, a surface loading of 0.018 atoms of gold per nm^2, equivalent to 480 mg/kg, in the solid was determined.

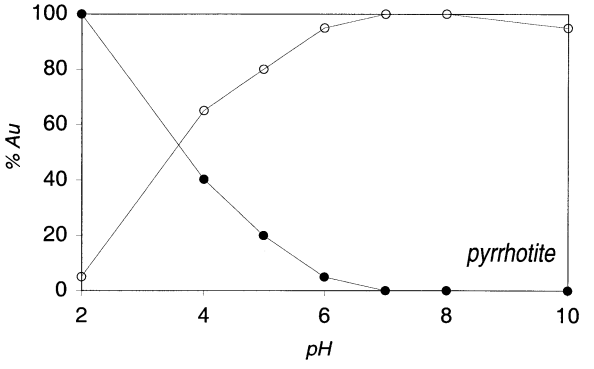

Fig. 6. Adsorption of gold(I) hydrosulphide complexes by synthetic pyrrhotite at 25°C. Percentage of total gold in solution (open circles) and adsorbed (filled circles) on pyrrhotite as a function of pH. For details, see "Experimental Methods."

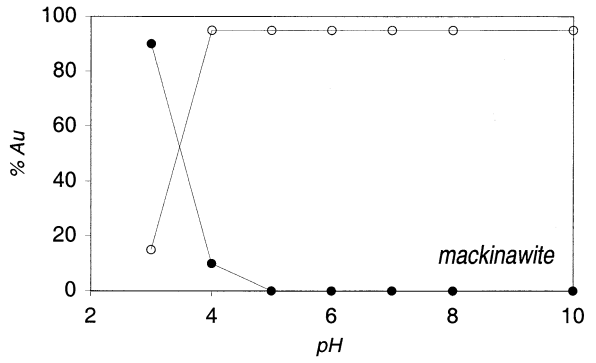

Fig. 7. Adsorption of gold(I) hydrosulphide complexes by synthetic mackinawite at 25°C. Percentage of total gold in solution (open circles) and adsorbed (filled circles) on mackinawite as a function of pH. For details, see "Experimental Methods."

The experiments with natural and synthetic pyrite at different gold concentrations show agreement within the experimental uncertainty. All iron sulphides show an adsorption of 90% or more at pH < 3. While the relative adsorption of mackinawite and pyrrhotite decreases quickly at higher pH and is zero at neutral pH, pyrite still adsorbs 90% of the gold from solution at pH $= 5$ and 30% at pH $= 10$. From the pH_{pzc} determination, no major differences in the surface charge of the three minerals, especially in solutions saturated with H_2S, can be expected, although the experiments show an enhanced sensitivity to AuHS° concentration for the iron monosulphide surfaces in comparison to that of the pyrite.

3.3. XPS Measurements

The potentiometric titrations provided some information about the charge on the surfaces as a function of pH. The adsorption experiments gave insight into the nature of removal of gold from aqueous solutions by the negatively charged surfaces as a function of pH. The question then arises as to the nature of the adsorbed gold on the sulphide mineral surfaces. Is the gold (in solution as hydrosulphide complexes) adsorbed and bonded to the different iron sulphide surfaces as surface complexes, or do chemisorption redox reactions occur leading to the reduction of Au^+ to Au° on the surface? To further elucidate the molecular basis for the adsorption of the gold complexes by these surfaces, we have therefore carried out XPS measurements.

XPS uses X-rays to eject core electrons from the surface atoms and measures the kinetic energy of the ejected atoms, thus permitting the determination of the electron binding energies. The p, d, and f levels become split upon ionisation, leading to vacancies in the $p_{1/2}$, $p_{3/2}$, $d_{3/2}$, $d_{5/2}$, $f_{5/2}$ and $f_{7/2}$ orbitals. Spin orbit splitting results in characteristic energy shifts and area ratios, which are orbital dependent (e.g., $p_{3/2}$ and $p_{1/2}$ have an area ratio of 2:1). In addition, the energy shifts are element sensitive (e.g., S 2p = 1.18 eV and Fe 2p = 13.1 eV).

XPS techniques have been widely used in the surface study of sulphide minerals. The main focus of the studies are mineral formation (Lennie et al., 1995), flotation (Buckley and Woods, 1984, 1985a, 1985b, 1987, 1995; Buckley et al., 1984; Nesbitt and Muir, 1994; Pratt et al., 1994; Mycroft et al., 1995a; Nesbitt et al., 1995, 1998; Vaughan et al., 1997), and adsorption (Bancroft and Jean, 1982; Jean and Bancroft, 1985, 1986; Bancroft et al., 1988; Hyland and Bancroft, 1989; Bancroft and Hyland, 1990; Mycroft et al., 1995b; Scaini et al., 1995, 1997, 1998; Maddox et al., 1996, 1998). Other often-used techniques to determine the chemical state of metal adsorbates at low to moderate concentration are Mössbauer spectroscopy and X-ray absorption spectroscopy (X-ray absorption near edge structure [XANES] and extended X-ray absorption fine structure [EXAFS]), whereas methods such as SIMS, scanning tunneling microscopy, atomic force microscopy, SEM, and Auger spectroscopy tend to have a rather image oriented focus.

More recently, Nesbitt et al. (1998) and Schaufuss et al. (1998a, 1998b) have studied pyrite surfaces using synchrotron radiation. They tuned the synchrotron radiation for maximal surface sensitivity (Seah and Dench, 1979) and explained their spectrum using a multiplet splitting model, suggesting that multiplet splitting of low-spin compounds may occur because of unsaturated bonds on the mineral surface, which cause iron to be in a high-spin state. This effect may be observed when using synchrotron radiation tuned to maximal surface sensitivity, but is minor in studies using conventional Mg K_α radiation as a source.

We have used XPS to study the nature of the adsorbed gold complexes and the oxidation state of iron and sulphur on the iron sulphide surfaces. Surfaces of natural pyrite and synthetic mackinawite enriched in adsorbed gold at pH $= 4$ have been studied. In the broad scan spectra of both pyrite and mackinawite, peaks of carbon, gold, iron, sodium, oxygen, silicon, sodium, and sulphur can be observed (Figs. 8 and 9).

3.4. Pyrite

The 2p spectrum of iron in pyrite is of diminished intensity (Fig. 10), and a three-point smoothing procedure was therefore applied, which clearly permits the determination of an electron binding energy of 707.05 eV for the Fe $2p_{3/2}$. This binding energy is within the range given by Buckley and Woods (1987) at 707 eV and by Lennie et al. (1996) at 707.2 eV (Table 3). Comparison of the iron peaks for pyrite and mackinawite suggests that the pyrite surface is depleted in iron, probably as a consequence of the cleaning of the mineral surface with acid before the adsorption experiment. By comparison, the sulphur 2p and iron 2p electron binding energies for vacuum fractured pyrite are little affected, but a few other minor contributions to the spectra, such as surface moieties of mono- and polysulphides observed in other studies (Nesbitt and Muir, 1994; Nesbitt et al., 1998; Schaufuss et al., 1998a; Nesbitt et al., 2000) could not be observed in the spectrum. The S $2p_{3/2}$ electron binding energy can be fitted best with one peak (Fig. 11) at 162.30 eV that lies within the range of other studies on pyrite which are summarised in Table 3. No additional peaks are found that would include the occurrence of surface polysulphides. Furthermore, no peaks are observed in the 165- to 170-eV range, which are characteristic of sulphur-oxygen moieties, as noted by Schaufuss et al. (1998a).

The main interest is focused on the chemical state of the Au ($4f_{7/2}$) electron binding energy and is based on a one peak fit at 84.8 eV (Figs. 12a and 12b). This value is in accordance with the study by Scaini et al. (1998). In their study of gold adsorp-

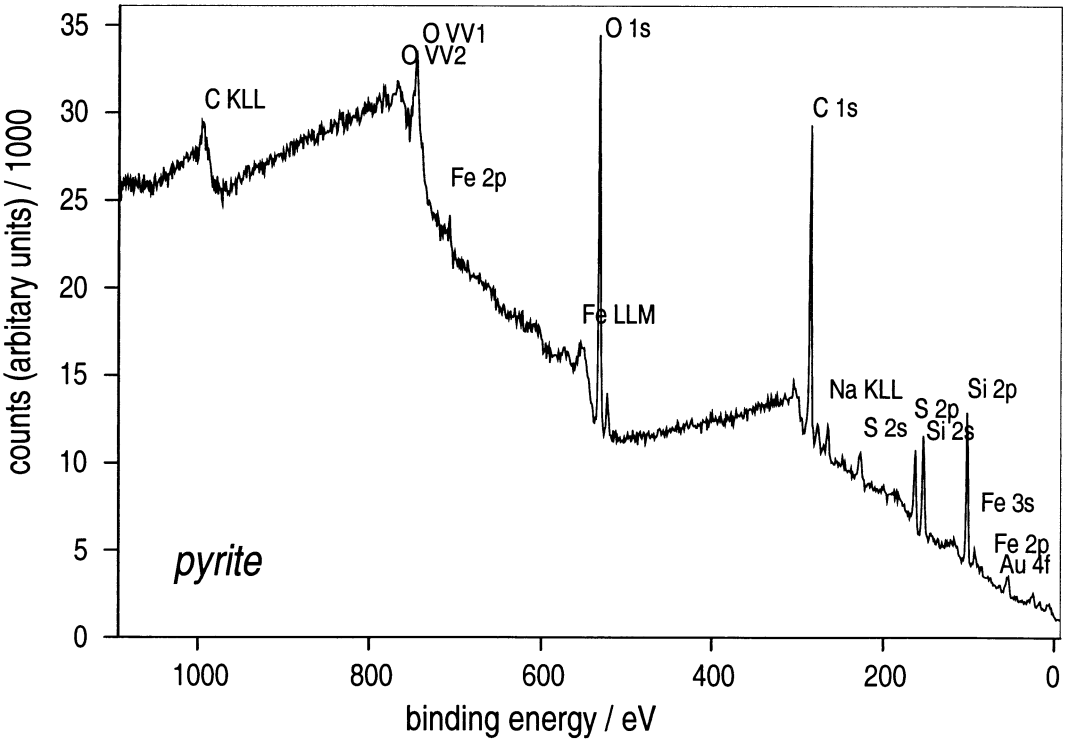

Fig. 8. The X-ray photoelectron spectroscopic spectrum of pyrite measured on a Sage Specs 100 system with nonmonochromatic Mg K_α (12 kV, 25 mA) radiation.

tion onto pyrite, they found (variable reaction time from 1 to 7 d at 25 and 90°C) gold compounds with binding energies of 84.7 to 85.1 eV and 84.0 eV (Table 4). The low energy peak (84.0 eV) was attributed to elemental gold (i.e., Au°), which was present in all but one of their experiments. The higher energy compound was determined by comparison with binding energies given by Van de Vondel et al. (1977) as a gold(I) surface complex. They studied gold(I) complexes with linear S-Au-S arrangements and found binding energies of 85.0 to 85.2 eV. Another possibility might have been the presence of Au clusters, which have been studied by Di Cenzo et al. (1988), but they have binding energies in the interval of 84.0 to 84.7 eV and cannot account for the higher values reported here and by Scaini et al. (1998). Our data are also consistent with the formation of Au(I) surface complexes, which have been identified on amorphous arsenic and antimony sulphides by Mössbauer spectroscopy (Cardile et al., 1993).

3.5. Mackinawite

Figure 13a shows the iron 2p electron binding energy spectrum of the synthetic mackinawite. Figure 13b shows the detail spectrum between 716.5 and 705.5 eV, and the observed peak attributed to the Fe $2p_{3/2}$ electron binding energy which shows an asymmetric broadening on the high-energy side. Several explanations can account for this. Herbert et al. (1998) studied poorly crystalline iron sulphides precipitated by sulphate reducing bacteria. By analogy to the spectroscopic studies of Pratt et al. (1994) on pyrrhotite, they used four symmetric peaks for mackinawite and three peaks for greigite to fit the spectrum and account for the peak shape. Three of the mackinawite peaks were attributed to multiplet splitting and one to a satellite. Gupta and Sen (1974, 1975) calculated the multiplet splitting of core 3p vacancy levels in transition metals compounds using a Hartree-Fock free ion approach. Their calculations give rise to a fit of one satellite and three peaks for the Fe_{2p} for Fe^{2+} and Fe^{3+} each.

However, in their study of freshly synthesised mackinawite, Lennie and Vaughan (1996) employed one peak with a wide tail to fit the spectrum. Their approach was based on Wertheim and Buchanan's (1977) study of semimetals and semiconductors, which showed that the formation of asymmetric peaks is a common feature due to excitation of the electrons at the Fermi surface for these substances. This phenomenon had been previously only described for metals and alloys. From the results of their earlier Mössbauer spectroscopic study of mackinawite, Kjekshus et al. (1972) had also proposed the delocalisation of electrons in the iron-containing layers. The distance between the iron atoms is 2.60 Å, which is just a little more than in the body-centred cubic form of iron with a distance of 2.59 Å.

The peak shape for mackinawite is accounted for by the delocalisation of the electrons in the iron layer and is approximated by one peak with a tail, which fits the data points quite accurately. The measured value of 707.3 eV coincides with the energy of the main peak determined by Herbert et al. (1998) in their three-peak multiplet model. The value is also consistent

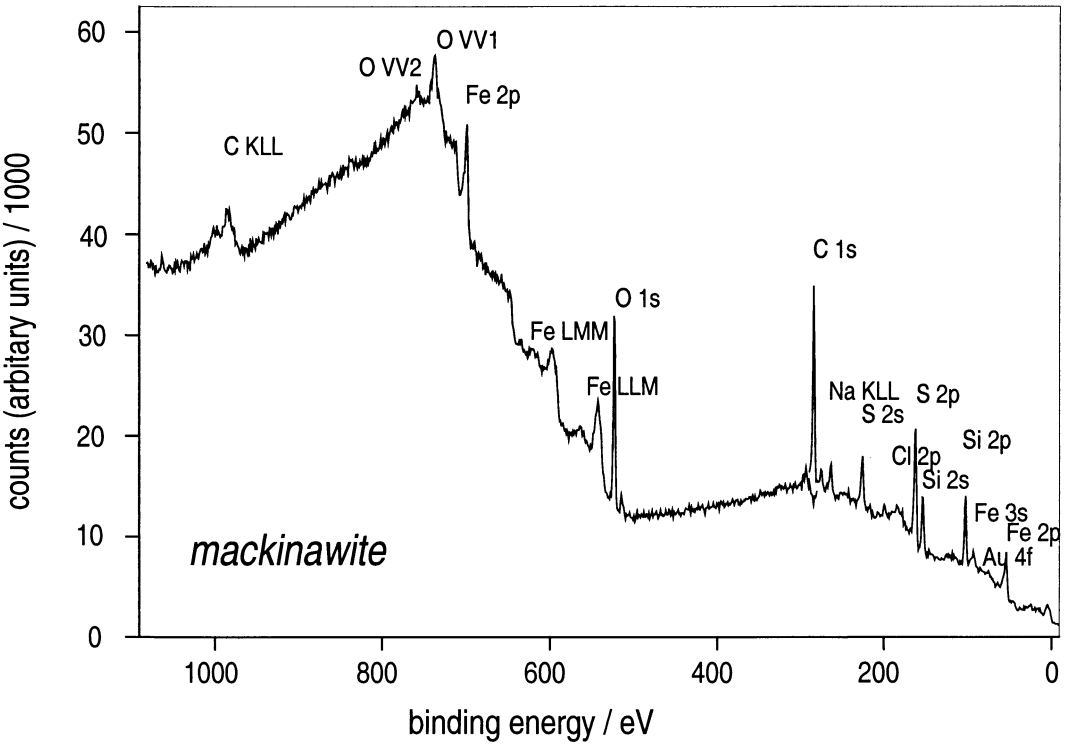

Fig. 9. The X-ray photoelectron spectroscopic spectrum of mackinawite measured on a Sage Specs 100 system with nonmonochromatic Mg K_α (12 kV, 25 mA) radiation.

with the study by Lennie et al. (1995), who proposed the tail model to fit their data.

For the S $2p_{3/2}$ peak, fitting was performed with 50:50 Gaussian-Lorentzian relation (Fig. 14), with the best fitting being achieved with two-peak set. This leads to peaks with full width at half maximum (FWHM) comparable to that found in other sulphide surface studies. The lower S $2p_{3/2}$ binding energy of 161.3 eV is intermediate between the value reported in the study of Herbert et al. (1998) (160.95 eV) and the higher value (161.82 eV) reported by Lennie and Vaughan (1996). The reason for the discrepancy between all three values may arise from the differences in the degree the crystallinity, which is indicated by the X-ray diffraction patterns and is a consequence of the method of synthesis. Studies on the synthesis of mackinawite have shown that the mixing of a sodium sulphide solution with a ferrous salt such as $FeSO_4 \cdot 6H_2O$ leads to a poorly crystalline precipitate (Berner, 1964, 1967). Mackinawite synthesised in this way is thus somewhat different from that formed by the reaction of sodium sulphide solution with iron wool at a known, buffered pH, as employed by Lennie et al. (1995). Differences in crystallinity can lead to changes in the stacking system of the (S-Fe-S) package layers. In a first step, single layers can be formed in which each sulphur may contain two additional protons. To enable the stacking, these protons have to be removed. Thus, the atomic environment around the sulphur is modified, which would cause a minor change in the binding energies. It should be noted that the value (161.3 eV) is more or less equivalent to the binding energies measured of pyrrhotite (161.1eV by Jones et al., 1992; 161.25 eV by Pratt et al., 1994; and 161.4 eV by Thomas et al., 1998).

The second peak with an S $2p_{3/2}$ electron binding energy of 162.90 eV is higher than values determined for pyrite (162.3 to 162.5 eV). Higher sulphur oxidation state compounds such as thiosulphates or sulphates have binding energies that are several electron volts higher (Table 5), as noted earlier. Surface H_2S on gold metal has been measured with a binding energy of 163 eV (Leavitt and Bebbe, 1994), but after drying in nitrogen atmosphere over silica gel, as in these experiments, surface-adsorbed H_2S is not expected. In addition, Jones et al. (1992) have proposed the formation of a surface Fe_2S_3 moiety with such a binding energy. They have studied the interaction of pyrrhotite with air, water, and perchloric acid and found a compound at a binding energy of 162.9 eV. This value, which cannot be attributed to either disulphide (S_2^{2-}; 162.2 to 162.5 eV) or to elemental sulphur (~164.2 to 164.35 eV), was interpreted as being due to an Fe_2S_3-like compound in an iron-depleted layer at the mineral surface. Such layers have been described as the result of selective removal of iron(III) hydroxides formed by the surface oxidation of iron sulphides (e.g., Sasaki et al., 1995) in combination with the formation of oxidised sulphur compounds. However, the reported X-ray data for the supposed Fe_2S_3 phase are in poor agreement (Schrader and Pietsch, 1969; Yamaguchi and Wada, 1973a, 1973b; Stiller et al., 1978; Sugiura, 1981; Sasaki et al., 1995). There is no reliable consensus as to its properties or whether such a phase has actually been synthesised.

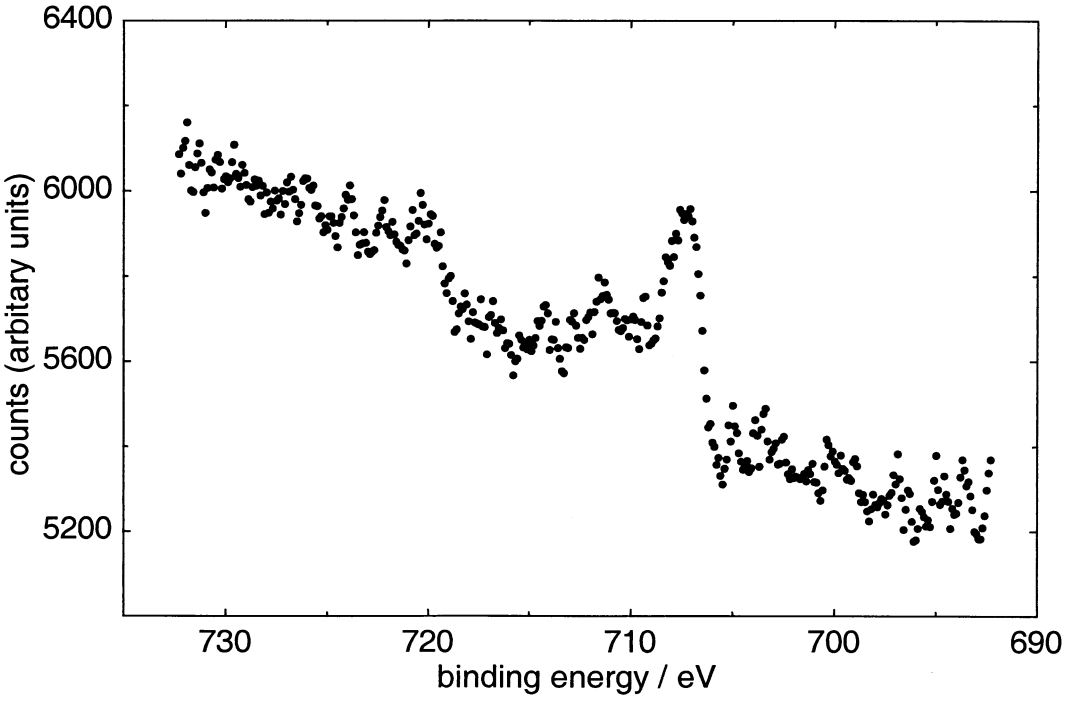

Fig. 10. X-ray photoelectron spectroscopic spectrum of the pyrite sample after reaction with gold(I) hydrosulphide solution at 25°C at pH 4: Fe 2p spectrum, which shows the separated Fe $2p_{3/2}$ (~720 eV) and Fe $2p_{1/2}$ (~707 eV) orbitals; because of the low signal-to-noise ratio, a three-point smoothing was applied.

Various studies (Table 5) have proposed S $2p_{3/2}$ binding energies for a variety of polysulphide compounds using the same apparatus with monochromatic aluminium radiation. These energies range from 163.0 to 163.6 eV binding energy, with extremes from 162 to 165.9 eV (Table 6) and the FWHMs varying from 0.95 to 2.2 eV. The variation is greater than could be attributed only to the variation of instrumental parameters and charging.

Table 3. S $2p_{3/2}$ and Fe $2p_{3/2}$ binding energies for iron sulphide compounds.

	Binding energy/eV			
Mineral	S $2p_{3/2}$	Fe $2p_{3/2}$	Charge correction	Source
Pyrite	162.3	707		Buckley and Woods (1987)
Pyrite	162.4	—		Bancroft and Hyland (1990)
Pyrite	162.4	—		Nesbitt and Muir (1994)
Pyrite	162.3	—		Knipe et al. (1995)
Pyrite	162.5 (50% G/50% L)	707.2	C 1s = 284.6	Lennie and Vaughan (1996)
Pyrite	162.3	707.05	C 1s = 284.6	This study
Greigite	—	709.15 (16.5%) 710.35 (8.8%) 711.39 (5%) 712.67 (1.7%)	C 1s = 285.0	Herbert et al. (1998)
Pyrrhotite $Fe_{0.98}S$	161.1	708		Buckey and Woods (1985a, 1985b)
Pyrrhotite Fe_7S_8	161.25	707.5		Pratt et al. (1994)
Mackinawite	161.82 (80% G/20% L)	707.25	C 1s = 284.6	Lennie and Vaughan (1996)
Mackinawite[a]	160.95	706.4 (14%) 707.3 (38.9%) 708.2 (13.2%) 713.3 (1.9%)[b]	C 1s = 285.0	Herbert et al. (1998)
Mackinawite	161.3	707.3	C 1s = 284.6	This study

[a] Herbert et al. (1998) used a triplet for mackinawite to fit the Fe $2p_{3/2}$ peak; area proportion in parentheses.
[b] Satellite.

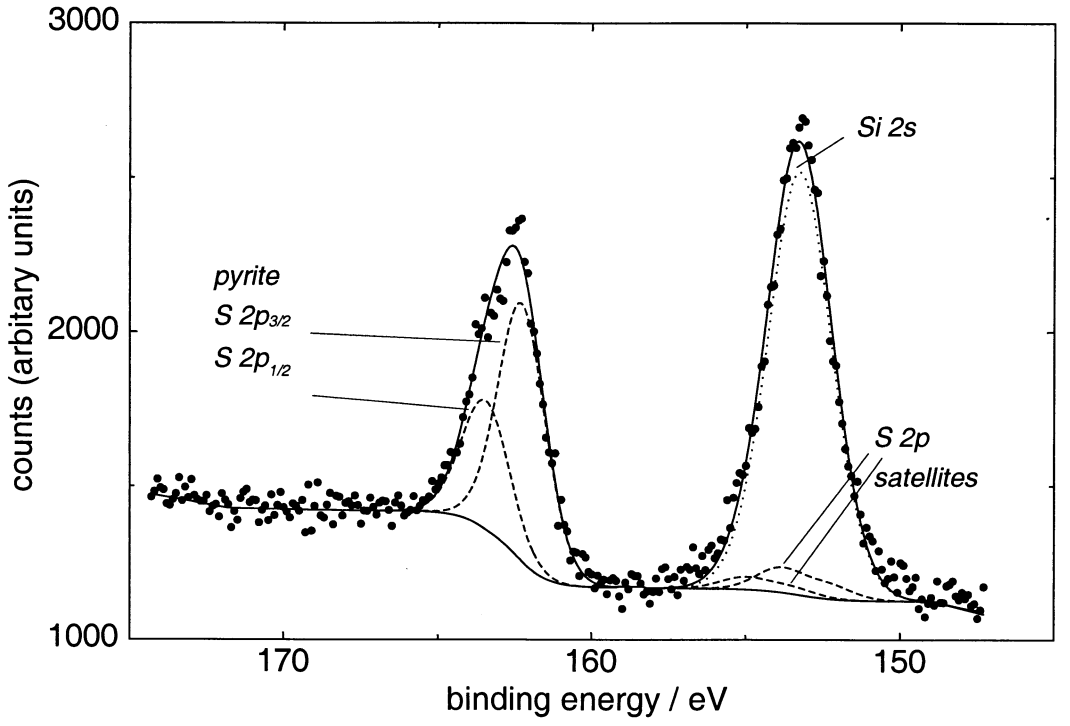

Fig. 11. S 2p/Si 2s X-ray photoelectron spectroscopic spectrum of the pyrite sample after reaction with gold(I) hydrosulphide solution at 25°C at pH 4: Upper solid line shows result of best fit, the lower being the background curve. Dashed lines are the S $2p_{3/2}$ and S $2p_{1/2}$ peaks at 162.3 and 163.45 eV. Their wider satellites at ~154.0 and 155.2 eV are contributions from Mg K_α and $K_{\alpha 4}$ arising from the nonmonochromatic source radiation; the dotted line is the Si 2s peak. Si contribution originates from the vacuum grease.

In considering the presence of polysulphide moieties on iron sulphide surfaces, the following points need to be taken into account:

- Polysulphides can show more than one single characteristic binding energy (Termes et al., 1987; Buckley et al., 1988).
- The variations in the binding energies permits the identification of at least "polysulphides" and "disulphides," if not even "monosulphides," when compared with literature data (Table 5).
- The longer the chain, the smaller the individual charges and the smaller the differences in distance of the central atom to its neighbour and hence an increasing similarity to the measured binding energies of S_8 rings or elemental sulphur.
- Instrumental resolution, even when using monochromatic

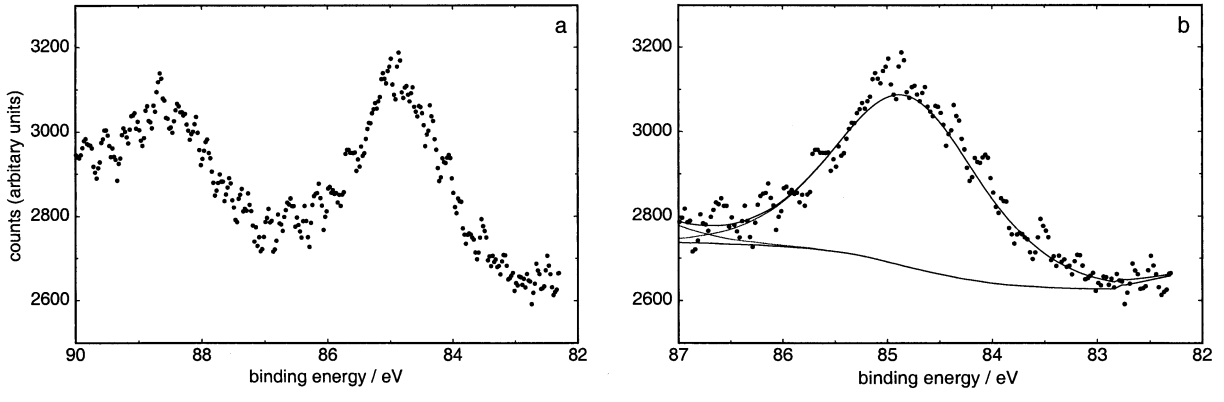

Fig. 12. X-ray photoelectron spectroscopic spectrum of the pyrite sample after reaction with gold(I) hydrosulphide solution at 25°C at pH 4: (a) Au 4f spectrum, which shows the separated Au $4f_{7/2}$ (~84 eV) and Au $4f_{5/2}$ (~87 eV) orbitals; and (b) detailed Au $4f_{7/2}$ spectrum with one symmetric peak fit. The upper solid line shows the upper total fit with added background, the lower the background fitted with the Shirley (1972) function.

Table 4. Au $4f_{7/2}$ binding energies for gold compounds.

Compound	Binding energy/eV	Source
Au (metallic)	83.9 to 84.0	Moulder et al. (1992)
Au clusters (5 to 7 atoms)	84.0 to 84.7	DiCenzo et al. (1988)
Compounds with linear S-Au-S arrangement[a]	85.0 /85.2	Van de Vondel et al. (1997)
Au(I) S surface complex	84.7 to 85.1	Scaini et al. (1998)
	84.8	This study
AuCl	86.2	Kishi and Ikeda (1974)
Au_2O_3	89.5	Aita and Tran (1991)
$Au(OH)_3$	91.3	Aita and Tran (1991)

[a] Charge correction with C 1s 285 eV.

radiation, might fail to resolve the individual peaks at least in low surface abundances.

- Fitting should include the area ratios based on the number of occurrences of an equivalent site within the chain.

Therefore, special care has to be taken in the fitting and interpretation of XPS spectra of sulphide surfaces containing compounds with binding energies of 163 to 164 eV.

Recent studies on pyrite using synchrotron XPS with a source energy of 200 eV (Bronold et al., 1994b; Schaufuss et al., 1998a; Nesbitt et al., 1998; Nesbitt and Muir, 1998) have observed variable binding energies due to surface groups, and these have been interpreted as the result of restructured surfaces and fractured bonds. This must also be taken into account when interpreting such spectra, especially when using methods with enhanced surface sensitivity (low angle, kinetic energy of ejected electrons of ~40 eV).

Preference is given to a polysulphide with one higher binding energy, as displayed in Figure 14. An attempt to fit the measured mackinawite S 2p spectrum with sets of predefined intensity ratios and a triplet with intensity of 1:2:2 corresponding to an H_2S_5 moiety led only to a minor improvement that was not statistically meaningful. Thus, a polysulphide species of short chain length with two to four sulphurs where the low energy peak would be indistinguishable from the monosulphide peak was preferred. The short chain length is proposed because the high-energy peak binding energy is still low in comparison to the other described polysulphides.

Although the concentration of the gold at the mineral surface is low, a good spatial energy resolution was achieved. The measured binding energy of 84.1 eV confirms the formation of metallic gold (83.9 to 84.0 eV; Fig. 15) on the mackinawite surface. Other compounds such as gold(III) chloride, sulphide, oxide, and hydroxide show distinctly higher binding energies (Table 4). The value of 84.1 eV has an inherent analytical uncertainty of 0.2 eV arising from the spectrometer calibration but confirms the formation of metallic gold or gold clusters of larger size (Di Cenzo et al., 1988).

3.6. Summary of Observations from the XPS Measurements

On the mackinawite and pyrite surfaces that were studied after gold adsorption, there was no evidence of formation of iron(III) oxide/hydroxide or sulphate that might have resulted

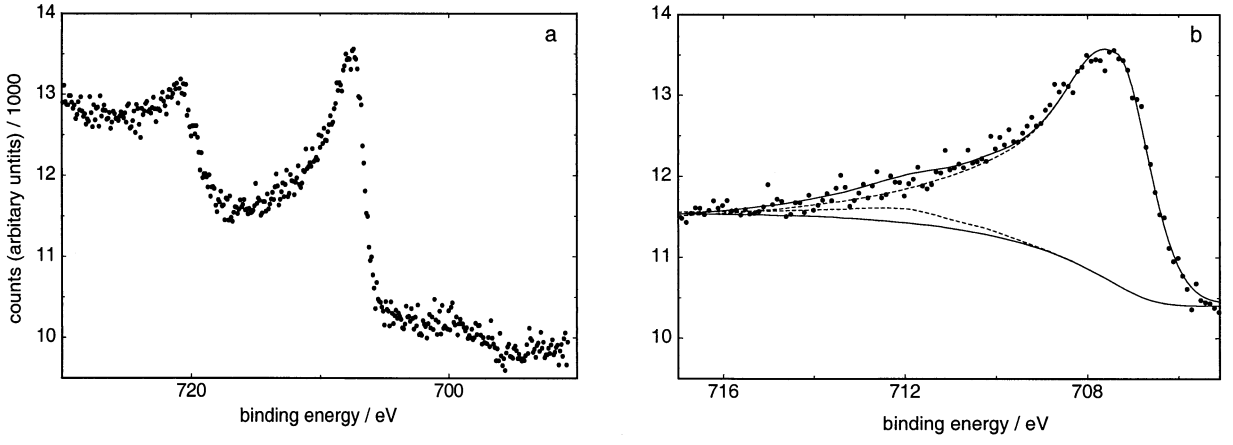

Fig. 13. X-ray photoelectron spectroscopic spectrum of the mackinawite sample after reaction with gold(I) hydrosulphide solution at 25°C at pH 4: (a) Fe 2p spectrum, which shows the separated Fe $2p_{3/2}$ (~720 eV) and Fe $2p_{1/2}$ (~707 eV) orbitals; and (b) detailed Fe $2p_{3/2}$ spectrum with one asymmetric peak fit. The upper solid line shows the upper total fit with added background, the lower the background fitted with the Shirley (1972) function. Dashed lines represent contributions to total fit: upper: primary fit; lower: satellite of primary line as correction for nonmonochromatic source (Mg $K_{\alpha 3,4}$ contribution).

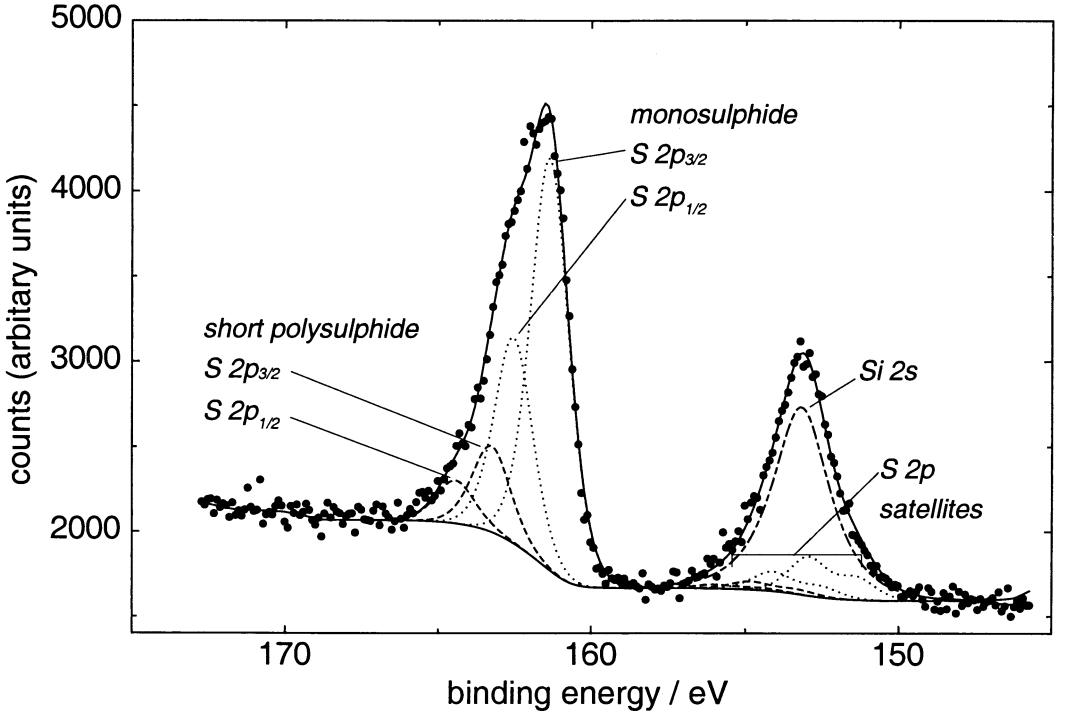

Fig. 14. S 2p/Si 2s X-ray photoelectron spectroscopic spectrum of the mackinawite sample after reaction with gold(I) hydrosulphide solution at 25°C and pH = 4: Upper solid line shows result of best fit, the lower being the background curve.

from atmospheric oxygen contamination. The pyrite shows electron binding energies for iron and sulphur that are typical of a freshly fractured, unoxidised surface. However, the XPS data for the mackinawite surface indicate a contribution from zero-valent sulphur, very probably in the form of a short-chain polysulphide having two to four sulphurs. Such polysulphide surface moieties may provide the initial precursor mechanism for the transform of reactive, metastable mackinawite to pyrite. Others (Berner et al., 1964, 1967; Schoonen and Barnes, 1991a, 1991b; Rickard and Luther, 1997; Benning et al., 2000; Cahill et al., 2000) have discussed the precursor role of mackinawite in the formation of pyrite.

The adsorption of hydrosulphidogold(I) complexes onto pyrite and mackinawite occurs quite differently for the two different surfaces. On pyrite, the measured Au $4f_{7/2}$ binding energy, 84.8 eV, is slightly lower than the range reported by Van de Vondel et al. (1977) (85.0 to 85.2 eV) but within the range determined by Scaini et al. (1998) (84.7 to 85.1 eV). The presence of Au^+ on the surface indicates that a surface complex has formed. Renders and Seward (1989b) also studied the adsorption of hydrosulphide complexes of Au^+ onto amorphous arsenic and antimony sulphide surfaces and confirmed the presence of linear, triatomic surface complexes using ^{197}Au Mössbauer spectroscopy (Cardile et al., 1993). These com-

Table 5. Selected S $2p_{3/2}$ binding energies for sulphur surface compounds.

		Binding energy/eV		
Surface compound	Substrate	S $2p_{3/2}$	Charge correction	Source
H_2S	Au	163	C 1s = 285	Leavitt and Bebbe (1994)
HS^-	Au	162.4	C 1s = 285	Leavitt and Bebbe (1994)
Monosulphide	Pyrite[a]	161.65	S 2p disulphide	Nesbitt and Muir (1994)
Disulphide	Mackinawite/greigite	162.2	C 1s = 285.0	Herbert et al. (1998)
Polysulphide	Mackinawite[a]/greigite[a]	163.15	C 1s = 285.0	Herbert et al. (1998)
Polysulphide	Various	163.01 to 163.6	S 2p disulphide	Details see Table 6
Sulphur	Pyrrhotite[a]	164.35	C 1s = 285.0	Pratt et al. (1994)
S_8	S_8	164.2	C 1s = 285.0	Lindberg et al. (1970)
Sulphite	Pyrrhotite[a]	164.35	C 1s = 285.0	Pratt et al. (1994)
Thio sulphate	Pyrite[a]	166.45	S 2p disulphide	Nesbitt and Muir (1994)
Sulphate	Pyrite[a]	168.25	S 2p disulphide	Nesbitt and Muir (1994)

[a] Formed by surface oxidation.

Table 6. S $2p_{3/2}$ binding energies with full width at half maximum (FWHM) of the peaks. The measured binding energies have been interpreted as polysulphide surface groups.

Author	Substrate	S $2p_{3/2}$	FWHM
		Binding energy/eV	eV
Hyland et al. (1989)[a]	Pyrite	163.2	1
Mycroft et al. (1990)[a]	Pyrite	163.3 to 163.7	—
De Donato et al. (1993)[b]	Pyrite (S_n)	165.3 to 165.9	1.6 to 1.8
Nesbitt and Muir (1994)[a]	Pyrite	163.6	2.2
Scaini (1995)[a]	Pyrite	163.5	—
Chaturvedi et al. (1996)[c]	Pyrite	164.1	—
Rinker et al. (1997)[a]	Marcasite	163.5 to 163.62	2.0
Nesbitt et al. (1995)[a]	Arsenopyrite	163.25	1.6
Pratt et al. (1994)[a]	Pyrrhotite	163.01	0.95 to 1.2
Pratt et al. (1994)[a]	Pyrrhotite	163.25	0.95 to 1.2
Thomas et al. (1998)[c]	Pyrrhotite	163.4	2.2
Herbert et al. (1998)[a]	Mackinawite/greigite	163.15	1.3
Legrand et al. (1998)[a]	Millerite	162 to 164	1.6

[a] All these samples were measured with the same equipment, using monochromatic Al Kα X-ray radiation at the University of Western Ontario.
[b] Nonmonochromatic Al Kα.
[c] Nonmonochromatic Mg Kα.

plexes form by adsorption of the neutral AuHS° complex onto the negatively charged pyrite surface to give ($=S_{\text{pyrite surface}} - [\text{Au-SH}]_{\text{adsorbed}}$). Ab initio calculations by Tossell (1996) have further confirmed the formation of such species on sulphide surfaces. We note also that Scaini et al. (1998) reported the presence of Au° together with Au^+ on pyrite surfaces similar to those studied in our experiments; however, we mention again that our experiments were conducted for $\leq$3 h with exclusion of both atmospheric oxygen and light. The presence of Au° on the pyrite surfaces studied by Scaini et al. (1998) suggests the photoreduction of Au^+ to Au° because of light contamination. Their adsorption experiments were conducted for times of up to 1 week, and despite the precautions taken to exclude light, their results strongly suggest the partial reduction of surface-complexed gold(I) to elemental gold. We have found no evidence for the reduction of Au^+ to Au° on the pyrite surface.

However, on the mackinawite surface, the XPS spectra indicate that all the gold is present only as Au°. The mackinawite surface is delicately poised in a redox sense and immediately undergoes oxidation by a strong oxidising agent such as Au^+. Hence, no gold(I) hydrosulphide surface complexes are preserved.

4. SUMMARY AND DISCUSSION

In this study, we have shown that the pH_{pzc} in solutions of variable ionic strength for pyrite, mackinawite, and pyrrhotite is at pH $<$ 3. This is in agreement with studies by Bebié et al. (1998) and Fornasiero et al. (1992), who studied pyrite and pyrrhotite surfaces using electrophoresis. Additionally, it could be shown that the pH_{pzc} is further reduced to values of pH $<$ 2 and not measurable using potentiometric titration, if the solution is H_2S saturated. This is consistent with the observation of Bebié et al. (1998) and further emphasises that H_2S and

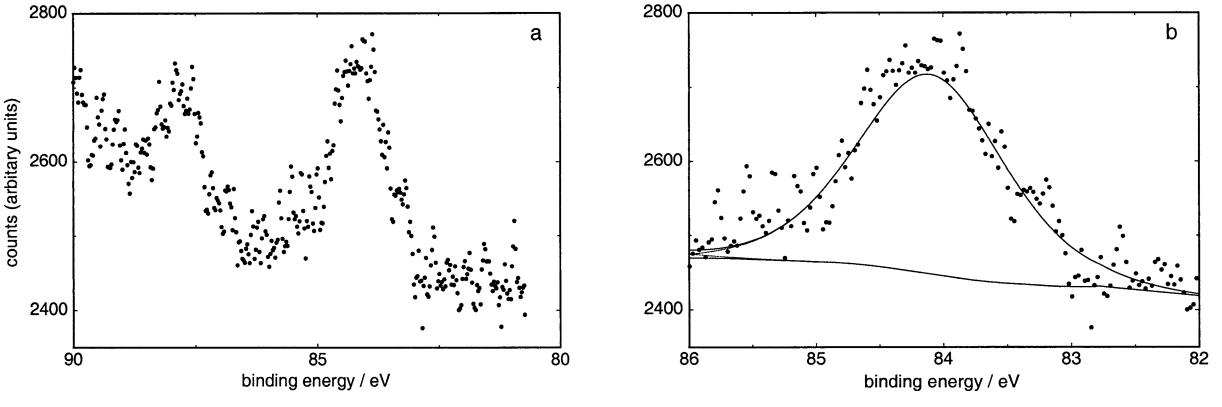

Fig. 15. X-ray photoelectron spectroscopic spectrum of the mackinawite sample after reaction with gold(I) hydrogensulphide solution at 25°C and pH 4: (a) Au 4f spectrum, which shows the separated Au $4f_{7/2}$ (~84 eV) and Au $4f_{5/2}$ (~87 eV) orbitals; and (b) detailed Au $4f_{7/2}$ spectrum with one symmetric peak fit. The upper solid line shows the upper total fit with added background, the lower is the background fitted with the Shirley (1972) function.

HS^- are potential determining species when considering sulphide mineral surfaces. Therefore, we have demonstrated that for our experiments over the whole pH interval from 2 to 10, the mineral surface is negatively charged. The adsorption experiments at 25°C (Figs. 6 and 7) using gold(I) hydrosulphide complexes and fresh, uncontaminated (by oxidation) mineral surfaces show that mackinawite and pyrrhotite have maximum adsorption at pH $\leq$ 3 and that their adsorption capacity rapidly decreases at higher pHs. However, the adsorption range for pyrite of both natural and synthetic origin extends to higher pH (Fig. 5). More than 90% of total gold is adsorbed pH $\leq$ 5. With increasing pH above 5, the adsorption of gold decreases to 30% at pH = 10. On pyrite, both the adsorbed solution species and the mineral surface itself show no change in the redox state. The gold $4f_{7/2}$ electron binding energy was determined to be 84.8 eV, which is consistent with previously reported values of Au(I) of Scaini et al. (1998), Maddox et al. (1998), and Mycroft et al. (1995b), who studied the reaction of gold(I) hydrosulphide and chloride complexes as well as gold(III) chloride with pyrite. Their studies also report the presence of Au° on pyrite as a result of reaction (adsorption) with gold(I) and gold(III) chloride and hydrosulphide species, which suggests possible light contamination and hence photoreduction of Au^+ or Au^{3+} to Au°.

In our experiments, only Au^+ was observed on the pyrite surfaces. The Au^+ is considered to be present as a surface complex, $FeSS_{pyrite}$ − Au-SH, formed by the adsorption of the uncharged AuHS°. Such a conclusion would be compatible with the findings of Renders and Seward (1989b) and Cardile et al. (1993), who demonstrated using ^{197}Au Mössbauer spectroscopy that the adsorption of AuHS° onto amorphous arsenic and antimony sulphide gave rise to the formation of a linear, triatomic surface complex. The pH region of highest adsorption of gold from aqueous sulphide solution onto both pyrite and mackinawite is also the low pH region (i.e., pH $\leq$ 3), in which the AuHS° is most stable and predominates (Renders and Seward, 1989b). Various sites occur on the pyrite surface (e.g., Guevremont et al., 1997, 1998) with which the AuHS° species may interact to form a surface complex. The nature of this process on a molecular level is unknown. In addition, the adsorption of AuHS° by arsenic(III)-containing natural pyrite is yet another process that has been little studied. The $Au(HS)_2^-$ complex becomes more stable in the near-neutral and alkaline pH region but is not considered to play a significant role in the adsorption of gold onto sulphide surfaces at pH > pH_{pzc} because of columbic repulsion. In contrast to pyrite, the XPS data indicate that the adsorption of AuHS° onto mackinawite results in the formation of Au° with no evidence of any remaining Au^+. Au^+ is an oxidising agent that is easily reduced on the reactive mackinawite surface with the associated oxidation of sulphide sulphur to zero-valent sulphur.

The geochemical implication arising from these experiments is that pyrite may act as a scavenger by removing gold from aqueous solution by surface adsorption mechanisms. If gold is transported in a hydrothermal ore fluid as hydrosulphidogold(I) complexes, then any process that decreases the activity of reduced sulphur, such as boiling or changes in the redox potential of the fluid (i.e., oxidation) with accompanying changes in pH as well as sulphide mineral deposition, may cause the deposition of gold. We have demonstrated that surface adsorption of gold(I) complexes by pyrite is also an important mechanism that has hitherto received little attention. In fact, the coupled process of pyrite precipitation that removes reduced sulphur from solution, causing gold deposition, combined with adsorption onto freshly forming pyrite surfaces, comprises an extremely effective gold concentrating mechanism.

Surface adsorption effects will be important in hydrothermal systems, but there is currently no information on the variation of surface charge (i.e., pH_{pzc}) of sulphide minerals in aqueous solutions at elevated temperatures and pressures. In addition, no experimentally based surface adsorption studies have been carried out under hydrothermal conditions. The adsorption of AuHS° by pyrite will extend to higher temperatures because this complex becomes more stable in near-neutral to alkaline conditions as pK_1 for H_2S (Suleimenov and Seward, 1997) increases to higher values.

There is evidence for the possible role of surface adsorption effects in determining the enrichment of gold in some gold-containing, natural, hydrothermal pyrite and arsenopyrite. Recent studies of natural, hydrothermal pyrite samples by Marion et al. (1991), Arehart et al. (1993), Cathelineau et al. (1989), and Genkin et al. (1998) on arsenopyrite have shown the existence of both submicroscopic, chemically bound Au^+ and elemental gold (i.e., Au°) using Mössbauer spectroscopy. Sha (1993) interpreted his XPS and SIMS data on gold-containing arsenian pyrite in terms of AuHS° adsorption. In addition, Simon et al. (1999a, 1999b) have studied pyrite from the Twin Creeks Carlin-type gold deposit and estimated that as much as 50% of the total gold at the deposit may have been removed from solutions unsaturated with respect to gold by adsorption processes. In their XANES and EXAFS study, they were able to discriminate between elemental and chemically bound Au^+ and to assign these to different mineralisation stages. It has been assumed that adsorbed Au(I) (e.g., Starling et al., 1989, Knipe et al., 1991, 1992) would react with time to form elemental gold (i.e., Au°); however, in this deposit and others, the gold(I) oxidation state has been preserved, and in fact, the gold(I)-containing pyrite is older than the pyrite with native gold. In an early stage of the formation of the above-mentioned deposit, subhedral to euhedral grains with arsenic concentrations of 0.33 to 0.85 wt.% and a gold content up to 60 mg/kg were formed at a temperature of ~250°C (Simon et al., 1999a). These samples showed an Au^0/Au^I ratio determined by XANES up to 0.052, which means that Au^+ or chemically bound gold dominates by far over Au°. In these samples, no individual gold grains have been observed in transmission electron microscopy, studies and the SIMS maps showed a homogeneous distribution. As the morphology of the pyrite suggests that crystallisation was slow, a sufficiently equilibrated surface of pyrite with the solution can therefore be assumed. Other pyrite grains from a different, later depositional stage have gold concentrations in the range of 595 to 1465 mg/kg. The XANES analysis gave an $Au°/Au^+$ ratio of 1.17 to 1.78, indicating that ~60% of the gold exists in the zero-valent state; the residual 40% is Au(I). Such grains apparently precipitated rapidly at 120 to 200°C.

The formation of pyrite in this lower temperature regime may also have some implications for gold scavenging from solutions. If the initial precursor in pyrite nucleation was an iron monosulphide phase, as has been suggested by Schoonen

and Barnes (1991c), then gold(I) complexes would be adsorbed and then reduced to Au°, as we have shown for mackinawite with the formation of surface polysulphide. This surface polysulphide could then act as a pyrite nucleation site. Further growth of pyrite would occur on the original seed material, and gold could then be adsorbed as AuHS° to form an Au(I) surface complex.

The entire field of surface chemistry, complex adsorption, and reaction by sulphide surfaces is poorly known at ambient temperature and essentially unknown under hydrothermal conditions. Further chemical insight into these important processes will come primarily from experimental studies. There is a desperate need for such data to better understand elemental scavenging in sulphide-containing systems over a wide range of ore-forming conditions.

Acknowledgments—This research was supported by the Swiss National Science Foundation (SNF) through SNF grant 20-46913.96 awarded to T. M. Seward. We are grateful to D. Günther and R. Frischknecht of the Institute of Isotope Geology and Mineral Resouces from the Eidgenössische Technische Hochschule (ETH) for the help with the ICP-MS measurements and A. Rossi-Elsner, I. Pfund-Klingenfuss, and M. Textor of the Laboratory of Surface Science and Technology of the ETH for help with the XPS analysis. We also thank D. Banerjee for his critical comments, as well as M. A. A. Schoonen and two anonymous reviewers for their helpful and constructive reviews of our manuscript.

Associate editor: S. A. Wood

REFERENCES

Aita C. R. and Tran C. T. (1991) Core level and valence band X-ray photoelectron spectroscopy of gold oxide. *J. Vacuum Sci. Technol. A.* **9,** 1498–1500.

Arakaki T. and Morse J. W. (1993) Coprecipitation and adsorption of Mn(II) with mackinawite (FeS) under conditions similar to those found in anoxic sediments. *Geochim. Cosmochim. Acta* **57,** 9–14.

Arehart G. B., Chryssoulis S. L., and Kesler S. E. (1993) Gold and arsenic in iron sulfides from sediment-hosted disseminated gold deposits: Implications for depositional processes. *Econ. Geol.* **88,** 171–185.

Bancroft G. M. and Jean G. E. (1982) Gold deposition at low temperature on sulphide minerals. *Nature* **298,** 730–731.

Bancroft G. M. and Hyland M. M. (1990) Spectroscopic studies of adsorption/reduction reactions of aqueous metal complexes on sulphide surfaces. *Rev. Min.* **23,** 511–558.

Bancroft G. M., Hyland M. M., and Kasrai M. (1988) High resolution XPS and XANES studies of metal ion reactions on sulphide surfaces. Abstracts of Papers—American Chemical Society, National Meeting. 196, Geoc65.

Beamson G. and Briggs D. (1992) *High Resolution XPS of Organic Polymers*. John Wiley, New York.

Bebié J., Schoonen M. A. A., Fuhrmann M., and Strongin D. R. (1998) Surface charge development on transition metal sulfides: An electrokinetic study. *Geochim. Cosmochim. Acta* **62,** 633–642.

Becker U., Hochella M. F., Jr., and Vaughan D. J. (1997) The adsorption of gold to galena surfaces: Calculation of adsorption/reduction energies, reaction mechanisms, XPS spectra and STM images. *Geochim. Cosmochim. Acta* **61,** 3565–3385.

Benning L. G. and Seward T. M. (1995) AuHS°—An important gold-transporting complex in high temperature hydrosulphide solutions. In *Water-Rock Interaction Conference—8* (eds. Y. K. Kharaka and O. V. Chudaev), pp. 783–786. Balkema Press, Rotterdam, the Netherlands.

Benning L. G. and Seward T. M. (1996) Hydrosulphide complexing of Au(I) on hydrothermal solutions form 150°-400°C and 150-1500 bar. *Geochim. Cosmochim. Acta* **60,** 1849–1871.

Benning L. G., Wilkin R. T., and Barnes H. L. (2000) reaction pathways in the Fe-S system below 100°C. *Chem. Geol.* **167,** 25–51.

Berner R. A. (1964) Iron sulphides formed from aqueous solution at low temperatures and atmospheric pressure. *J. Geol.* **72,** 826–834.

Berner R. A. (1967) Thermodynamic stability of sedimentary iron sulfides. *Am. J. Sci.* **265,** 773–785.

Briggs D. and Rivière J. C. (1983) Spectra interpretation. In *Practical Surface Analysis by Auger and X-Ray Photoelectron Spectroscopy*, pp. 87–140. John Wiley, New York.

Bronold M., Tomm Y., and Jaegermann W. (1994a) Surface states on cubic d-band semiconductor pyrite (FeS_2). *Surf. Sci.* **314,** L931–L936.

Bronold M., Pettenkofer C., and Jaegermann W. (1994b) Surface photovoltage measurements on pyrite (100) cleavage planes—Evidence for electronic bulk defects. *J. Appl. Phys.* **76,** 5800–5808.

Buckley A. N. and Woods R. (1984) An X-ray photoelectron spectroscopic investigation of the surface oxidation of sulfide minerals. *J. Electrochem. Soc.* **131,** C99–C99.

Buckley A. N. and Woods R. (1985a) X-ray photoelectron-spectroscopy of oxidized pyrrhotite surfaces. 2. Exposure to aqueous-solutions. *Appl. Surf. Sci.* **20,** 472–480.

Buckley A. N. and Woods R. (1985b) *X-ray photoelectron-spectroscopy of oxidized pyrrhotite surfaces. 1. Exposure to air. Appl. Surf. Sci.* **22/23,** 280–287.

Buckley A. N. and Woods R. (1987) The surface oxidation of pyrite. *Appl. Surf. Sci.* **27,** 437–452.

Buckley A. N. and Riley K. W. (1991) Self-induced floatability of sulfide minerals—Examination of recent-evidence for elemental sulfur as the hydrophobic entity. *Surf. Interface Anal.* **17,** 655–659.

Buckley A. N. and Woods R. (1995) Identifying chemisorption in the interaction of thiol collectors with sulfide minerals by XPS: Adsorption of xanthate on silver and silver sulfide. *Coll. Surf.* **104,** 295–305.

Buckley A. N. and Woods R. (1997) Chemisorption—The thermodynamically favoured process in the interaction of thiol collectors with sulphide minerals. *Int. J. Min. Proc.* **51,** 15–26.

Buckley A. N., Hamilton I. C., and Woods R. (1984) Investigation of the surface oxidation of bornite by linear potential sweep voltammetry and X-ray photoelectron- spectroscopy. *J. Appl. Electrochem.* **14,** 63–74.

Buckley A. N., Wouterlood H. J., Cartwright P. S., and Gillard R. D. (1988) Core electron binding energies of platinum and rhodium polysulfides. *Inorg. Chim. Acta* **143,** 77–80.

Cahill C. L., Benning L. G., Barnes H. L., and Parise J. B. (2000). In situ time-resolved X-ray diffraction of iron sulfides during hydrothermal pyrite growth. *Chem. Geol.* **167,** 53–63.

Cardile C. M., Cashion J. D., McGrath A. C., Renders P. J., and Seward T. M. (1993) ^{197}Au Mossbauer study of Au_2S and gold adsorbed onto As_2S_3 and Sb_2S_3 substrates. *Geochim. Cosmochim. Acta* **57,** 2481–2486.

Cathelineau M., Boiron M.-C., Holliger P., Marion P., and Denis M. (1989) Gold in arsenopyrites: Crystal chemistry, location and state, physical and chemical conditions of deposition. *Econ. Geol. Monogr.* **6,** 328–341.

Chander S., Wie J. M., and Fuerstenau D. W. (1975) On the native floatability and surface properties of naturally hydrophobic solids. *AIChE Symp. Ser.* **150,** 183–188.

Chaturvedi S., Katz R., Guevremont J., Schoonen M. A. A., and Strongin D. R. (1996) XPS and LEED study of a single-crystal surface of pyrite. *Am. Min.* **81,** 261–264.

Cody G. D., Boctor N. Z., Filley T. R., Hazen R. M., Scott J. H., Sharma A., and Yoder H. S., Jr. (2000). Primodial carbonylated iron-sulfur compounds and the synthesis of pyruvate. *Science* **289,** 1337–1340.

Dasbach R., Willeke G., and Blenk O. (1993) Iron sulphide for photovoltaics. *MRS Bull.* **18,** 56–60.

Davidson W. (1991) The solubility of irons sulphides in synthetic and natural waters at ambient temperature. *Aquat. Sci.* **53,** 309–329.

De Donato P., Mustin C., Benoit R., and Erre R. (1993) Spatial distribution of iron and sulphur species on the surface of pyrite. *Appl. Surf. Sci.* **68,** 81–93.

Dekkers M. J. and Schoonen M. A. A. (1994) An electrokinetic study of synthetic greigite and pyrrhotite. *Geochim. Cosmochim. Acta* **58,** 4147–4153.

Di Cenzo S. B., Berry S. D., and Hartford E. H. J. (1988) Photoelectron

spectroscopy of single size Au clusters collected on a substrate. *Phys. Rev. B.* **38,** 465–468.

Drobner E., Huber H., Wächtershäuser G., Rose D., and Stetter K. O. (1990) Pyrite formation linked with hydrogen evolution under anaerobic conditions. *Nature* **346,** 742–744.

Dzombak D. A. and Morel F. M. M. (1990) *Surface Complexation Modeling—Hydrous Ferric Oxide*. John Wiley, New York.

Eggleston C. M. and Hochella M. F., Jr. (1993) Tunneling spectroscopy applied to PbS (100) surfaces: Fresh surfaces, oxidation and sorption of aqueous gold. *Am. Mineral.* **78,** 877–883.

Fornasiero D., Eijt V., and Ralston J. (1992) An electrokinetic study of pyrite oxidation. *Coll. Surf.* **62,** 63–73.

Genkin A. D., Bortnikov N. S., Cabri L. J., Wagner F. E., Stanley C. J., Safonov Y. G., McMahon G., Friedl J., Kerzin A. L., and Gamyanin G. N. (1998) A multidisciplinary study of invisible gold in arsenopyrite from four mesothermal gold deposits in Siberia, Russian Federation. *Econ. Geol.* **93,** 463–487.

Guevremont J. M., Strongin D. R., and Schoonen M. A. A. (1997) Effects of surface imperfections on the binding of CH_3OH and H_2O on FeS_2 (100) using adsorbed Xe as a probe of mineral structure. *Surf. Sci.* **391,** 109–124.

Guevremont J. M., Strongin D. R., and Schoonen M. A. A. (1998) Photoemission of adsorbed xenon, X-ray photoelectron spectroscopy and temperature-programmed desorption studies of H_2O on FeS_2 (100). *Langmuir* **14,** 1361–1366.

Gupta R. P. and Sen S. K. (1974) Calculation of multiplet structure of core p-vacancy levels. *Phys. Rev. B.* **10,** 71–77.

Gupta R. P. and Sen S. K. (1975) Calculation of multiplet structure of core p-vacancy levels. II. *Phys. Rev. B.* **12,** 15–19.

Hannington M. D. and Scott S. D. (1989) Gold mineralization in volcanogenic massive sulfides: Implications of data from active hydrothermal vents on the modern sea floor. *Econ. Geol. Mono.* **6,** 491–507.

Hannington M. D., Peter J. M., and Scott S. D. (1986) Gold in sea-floor polymetallic sulfide deposits. *Econ. Geol.* **81,** 1867–1883.

Hannington M. D., Herzig P. M., and Scott S. D. (1991) Auriferous hydrothermal precipitates on the modern seafloor. In *Gold Metallogeny and Exploration* (ed. R. P. Foster), pp. 249–282. Blackie and Son Ltd., London.

Healy T. W. and Moignard M. S. (1976) A review of electrokinetic studies of metal sulphides. In *Flotation: A. M. Gaudin Memorial Volume* (ed. M. C. Fuerstenau), pp. 275–297. American Institute of Mining, Metallurgical, and Petroleum Engineers, New York.

Heinrich C. A. and Seward T. M. (1990) A spectrophotometric study of aqueous iron(II) chloride complexing from 25 to 200°C. *Geochim. Cosmochim. Acta* **54,** 2207–2221.

Herbert R. B. J., Benner S. G., Pratt A. R., and Blowes D. W. (1998) Surface chemistry and morphology of poorly crystalline iron sulfides precipitated in media containing sulphate-reducing bacteria. *Chem. Geol.* **144,** 87–97.

Herzig P. M. and Hannington M. D. (1995) Hydrothermal activity, vent fauna, and submarine gold mineralization at the alkaline fore-arc seamounts near Lihir Island, Papua New Guinea. In *Proceedings PACRIM '95*, pp. 279–284.

Herzig P. M., Hannington M. D., Fouquet Y., Von Stackelberg U., and Petersen S. (1993) Gold-rich polymetallic sulfides from the Lau back arc and implications for the geochemistry of gold in sea-floor hydrothermal systems of the Southwest Pacific. *Econ. Geol.* **88,** 2182–2209.

Hyland M. M. and Bancroft G. M. (1989) An XPS study of gold deposition at low temperatures on sulphide minerals: reducing agents. *Geochim. Cosmochim. Acta* **53,** 367–372.

Jean G. E. and Bancroft G. M. (1985) An XPS and SEM study of gold deposition at low temperatures on sulphide mineral surfaces: Concentration of gold by adsorption/reduction. *Geochim. Cosmochim. Acta* **49,** 979–987.

Jean G. E. and Bancroft G. M. (1986) Heavy metal adsorption by sulphide mineral surfaces. *Geochim. Cosmochim. Acta* **50,** 1455–1463.

Jones C. F., LeCount S., Smart R. S. C., and White T. (1992) Compositional and structural alteration of pyrrhotite surfaces in solution: XPS and XRD studies. *Appl. Surf. Sci.* **55,** 65–85.

Kelebek S. and Smith G. W. (1989) Electrokinetic properties of a galena and chalcopyrite with the collectorless flotation behaviour. *Coll. Surf.* **40,** 137–143.

Kishi K. and Ikeda S. (1974) X-ray photoelectron spectroscopic study of the reaction of evaporated metal films with chlorine gas. *J. Phys. Chem.* **78,** 107–112.

Kjekshus A., Nicholson D. G., and Mukherjee A. D. (1972) On the bonding in tetragonal FeS. *Acta Chem. Scand.* **26,** 1105–1110.

Knipe S. W., Foster R. P., and Stanley C. J. (1991) Hydrothermal precipitation of precious metals on sulfide substrates. In *Brazil Gold '91*, pp. 431–435.

Knipe S. W., Foster R. P., and Stanley C. J. (1992) Role of sulphide surfaces in sorption of precious metals from hydrothermal fluids. *Trans. Inst. Min. Metal. Sec. B.* **101,** 83–88.

Knipe S. W., Mycroft J. R., Pratt A. R., Nesbitt H. W., and Bancroft G. M. (1995) X-ray photoelectron spectroscopy study of water adsorption on iron sulphide minerals. *Geochim. Cosmochim. Acta* **59,** 1079–1090.

Kornicker W. A. and Morse J. W. (1991) Interactions of divalent cations with the surface of pyrite. *Geochim. Cosmochim. Acta* **55,** 2159–2171.

Leavitt A. J. and Bebbe T. P. J. (1994) Chemical reactivity of studies of hydrogen sulfide on Au (111). *Surf. Sci. Incl. Surf. Sci. Lett.* **314,** 23–33.

Legrand D. L., Nesbitt H. W., and Bancroft G. M. (1998) X-ray photoelectron spectroscopic study of a pristine millerite (NiS) surface and the effect of air and water oxidation. *Am. Min.* **83,** 1256–1265.

Lennie A. R. and Vaughan D. J. (1992) Kinetics of the marcasite-pyrite transformation: An infrared spectroscopic study. *Am. Min.* **77,** 1166–1171.

Lennie A. R. and Vaughan D. J. (1996) Spectroscopic studies of iron sulfide formation and phase relations at low temperatures. In *Mineral Spectroscopy: A Tribute to Roger G. Burns* (eds. M. D. Dyar, C. McCammon, and M. W. Schaefer), pp. 117–131. Geochemical Society, University Park, PA.

Lennie A. R., Redfern S. A. T., Schofield P. F., and Vaughan D. J. (1995) Synthesis and Rietveld crystal structures refinement of mackinawaite, tetragonal FeS. *Mineral. Mag.* **59,** 677–683.

Lindberg B. J., Hamrin K., Johansson G., Gelius U., Fahlman A., Nordling C., and Siegbahn K. (1970) Molecular spectroscopy by means of ESCA. *Phys. Scripta* **1,** 286–298.

Luther G. W. (1991) Pyrite synthesis via polysulphide compounds. *Geochim. Cosmochim. Acta* **55,** 2839–2849.

Maddox L. M., Bancroft G. M., and Lorimer J. W. (1996) Interaction of aqueous silver ions with the surface of pyrite. *J. Appl. Electrochem.* **26,** 1185–1193.

Maddox L. M., Bancroft G. M., Scaini M. J., and Lorimer J. W. (1998) Invisible gold: Comparison of Au deposition on pyrite and arsenopyrite. *Am. Min.* **83,** 1240–1245.

Marion P., Monroy M., Holliger P., Boiron M.-C., Cathelineau M., Wagner F. E., and Friedl J. (1991) Gold bearing pyrites: A combined ion microprobe and Mossbauer spectrometry approach. In *Transport and Deposition of Metals* (eds. M. Pagel and J. L. Leroy), pp. 677–680. CNRS CREGU, Vandoeuvre les Nancy, France.

Mirnov A. G., Zhmodik S. M., and Maksimova E. A. (1981) An experimental investigation of the sorption of gold by pyrites with different thermoelectric properties. *Geochem. Intern.* **18,** 153–160.

Morse J. W. and Arakaki T. (1993) Adsorption and coprecipitation of divalent metals with mackinawite (FeS). *Geochim. Cosmochim. Acta* **57,** 3635–3640.

Morse J. W., Millero F. J., Cornwell J. C., and Rickard D. T. (1987) The chemistry of the hydrogen sulfide and iron sulfide systems in natural waters. *Earth. Sci. Rev.* **24,** 1–42.

Moulder J. F., Stickle W. F., Sobol P. E., and Bomben K. D. (1992) *Handbook of X-Ray Photoelectron Spectroscopy (A Reference Book of Standard Spectra for Identification and Interpretation of XPS Data)*. Perkin-Elmer Corporation, Norwalk, CT.

Moyle A. J., Doyle B. J., Hoogvliet H., and Ware A. R. (1990) Ladolam gold deposit, Lihir Island. In *Geology of the Mineral Deposits of Australia and Papua New Guinea* (ed. F. E. Hughes), pp. 1793–1805. Australia Institute of Mining and Metallurgy, Carlton.

Mycroft J. R., Bancroft G. M., McIntyre N. S., Lorimer J. W., and Hill I. R. (1990) Detection of sulphur and polysulphides on electrochem-

ically oxidized surfaces by X-ray photoelectron spectroscopy and Raman spectroscopy. *J. Electroanal. Chem.* **292,** 139–152.

Mycroft J. R., Bancroft G. M., McIntyre N. S., and Lorimer J. W. (1995a) Spontaneous deposition of gold on pyrite from solution containing Au(III) and Au(I) chlorides: Part I, a surface study. *Geochim. Cosmochim. Acta* **59,** 3351–3365.

Mycroft J. R., Nesbitt H. W., and Pratt A. R. (1995b) X-ray photoelectron and Auger electron spectroscopy of air-oxidized pyrrhotite: Distribution of oxidized species with depth. *Geochim. Cosmochim. Acta* **59,** 721–733.

Nesbitt H. W. and Muir I. J. (1994) X-ray photoelectron spectroscopic study of a pristine pyrite surface reacted with water vapour and air. *Geochim. Cosmochim. Acta* **58,** 4667–4679.

Nesbitt H. W. and Muir I. J. (1998) Oxidation states and speciation of secondary products on pyrite and arsenopyrite reacted with mine waste waters and air. *Mineral. Petrol.* **62,** 123–144.

Nesbitt H. W., Muir I. J., and Pratt A. R. (1995) Oxidation of arsenopyrite by air and air-saturated, distilled water, and implications for mechanism of oxidation. *Geochim. Cosmochim. Acta* **59,** 1773–1786.

Nesbitt H. W., Bancroft G. M., Pratt A. R., and Scaini M. J. (1998) Sulfur and iron surface states on fractured pyrite surfaces. *Am. Min.* **83,** 1067–1076.

Nesbitt H. W., Scaini M., Höchst H., Bancroft G. M., Schaufuss A. G., and Szargan R. (2000) Synchrotron XPS evidence for Fe^{2+}-S and Fe^{3+}-S surface species on pyrite fracture surfaces and their 3D electronic states. *Am. Mineral.* **85,** 850–857.

Ney P. (1973) Zeta-Potentiale und Flotierbarkeit von Mineralien. In *Applied Mineralogy/Technische Mineralogie, Vol. 6* (eds. A. Fréchette, H. Kirsch, L. B. Sand, and F. Trojer), pp. 215. Springer-Verlag, Berlin, Germany.

Pan P. and Wood S. A. (1994) Solubility of Pt and Pd-sulfides and Au metal in aqueous sulfide solutions: II. Results at 200°-350°C and saturated vapour pressure. *Min. Deposita* **29,** 373–390.

Parks G. A. and De Bruyn P. L. (1962) The zero point of charge of oxides. *J. Phys. Chem.* **66,** 967–973.

Pratt A. R., Muir I. J., and Nesbitt H. W. (1994) X-ray photoelectron and Auger electron spectroscopic studies of pyrrhotite and mechanism of air oxidation. *Geochim. Cosmochim. Acta* **58,** 827–841.

Pro Fit 5.1 user's manual. (1999) QuantumSoft, Zürich, Switzerland.

Renders P. J. and Seward T. M. (1989a) The stability of hydrosulphido- and sulphido-complexes of Au(I) and Ag(I) at 25°C. *Geochim. Cosmochim. Acta* **53,** 245–253.

Renders P. J. and Seward T. M. (1989b) The adsorption of thio gold(I) complexes by amorphous As_2S_3 and Sb_2S_3 at 25 and 90°C. *Geochim. Cosmochim. Acta* **53,** 255–267.

Rickard D. T. (1969) The chemistry of iron sulphide formation at low temperatures. *Stock. Contrib. Geol.* **20,** 67–95.

Rickard D. T. (1975) Kinetics and mechanism of pyrite formation at low temperatures. *Am. J. Sci.* **275,** 636–652.

Rickard D. T. (1989) Experimental concentration-time curves for the iron(II) sulphide precipitation process in aqueous solutions and their interpretation. In *Kinetic Geochemistry* (eds. J. Schott and A. C. Lasaga), pp. 315–324. Elsevier, Amsterdam, the Netherlands.

Rickard D. T. (1997) Kinetics of pyrite formation by the H_2S oxidation of iron (II) monosulfide in aqueous solutions between 25 and 125°C: The rate equation. *Geochim. Cosmochim. Acta* **61,** 115–134.

Rickard D. T. and Luther G. W. (1997) Kinetics of pyrite formation by the H_2S oxidation of iron(II) monosulfide in aqueous solutions between 25 and 125°C: The mechanism. *Geochim. Cosmochim. Acta* **61,** 135–147.

Rinker M. J., Nesbitt H. W., and Pratt A. R. (1997) Marcasite oxidation in low-temperature acidic (pH 3.0) solutions: Mechanism and rate laws. *Am. Min.* **82,** 900–912.

Russell M. J. and Hall A. J. (1997) The emergence of life from iron monosulphide bubbles at a submarine hydrothermal redox and pH front. *J. Geol. Soc. Lond.* **154,** 377–402.

Russell M. J., Daniel R. M., Hall A. J., and Sherringham J. A. (1994) A hydrothermally precipitated catalytic iron sulphide membrane as first step towards life. *J. Mol. Evol.* **39,** 231–243.

Sasaki K., Tsunekawa M., Ohtsuka T., and Konno H. (1995) Confirmation of a sulfur-rich layer on pyrite after oxidative dissolution by Fe(III) ions around pH 2. *Geochim. Cosmochim. Acta* **59,** 3155–3158.

Scaini M. J., Bancroft G. M., Lorimer J. W., and Maddox L. M. (1995) The interaction of aqueous silver species with sulphur-containing minerals as studied by XPS, AES, SEM, and electrochemistry. *Geochim. Cosmochim. Acta* **59,** 2733–2747.

Scaini M. J., Bancroft G. M., and Knipe S. W. (1997) An XPS, AES, and SEM study of the interactions of gold and silver chloride species with PbS and FeS_2: Comparison to natural samples. *Geochim. Cosmochim. Acta* **61,** 1223–1231.

Scaini M. J., Bancroft G. M., and Knipe S. W. (1998) Reactions of aqueous Au^{1+} sulfide species with pyrite as a function of pH and temperature. *Am. Min.* **83,** 316–322.

Schaufuss A. G., Nesbitt H. W., Kartio I., Laajalehto K., Bancroft G. M., and Szargan R. (1998a) Reactivity of surface chemical states on fractured pyrite. *Surf. Sci.* **411,** 321–328.

Schaufuss A. G., Nesbitt H. W., Kartio I., Laajalchto K., Bancroft G. M., and Szargan R. (1998b) Incipient oxidation of fractured pyrite surfaces in air. *J. Electron. Spec. Rel. Phen.* **96,** 69–82.

Schoonen M. A. A. and Barnes H. L. (1988) An approximation of the second dissociation constant for H_2S. *Geochim. Cosmochim. Acta* **52,** 649–654.

Schoonen M. A. A. and Barnes H. L. (1991a) Reactions forming pyrite and marcasite from solution: I. Nucleation of FeS_2 below 100°C. *Geochim. Cosmochim. Acta* **55,** 1495–1504.

Schoonen M. A. A. and Barnes H. L. (1991b) Reactions forming pyrite and marcasite from solution: II. Via FeS precursors below 100°C. *Geochim. Cosmochim. Acta* **55,** 1505–1514.

Schoonen M. A. A. and Barnes H. L. (1991c) Mechanisms of pyrite and marcasite formation from solution: III. Hydrothermal processes. *Geochim. Cosmochim. Acta* **55,** 3491–3504.

Schoonen M. A. A. and Barnes H. L. (1991d) Erratum to mechanisms of pyrite and markasite formation from solution: III. Hydrothermal processes. *Geochim. Cosmochim. Acta* **56,** 2131.

Schoonen M. A. A., Fisher N. S., and Wente M. (1992) Gold sorption onto pyrite and goethite: A radiotracer study. *Geochim. Cosmochim. Acta* **56,** 1801–1814.

Schrader R. and Pietsch C. (1969) Über amorphes und kristallines Eisen(III)-sulfid. *Kristall und Technik* **4,** 385–397.

Seah M. P. and Dench W. A. (1979) Quantitative electron spectroscopy of surfaces: A standard data base fore electron inelastic mean free path in solids. *Surf. Interface Anal.* **1,** 2–11.

Seward T. M. (1973) Thio complexes of gold and the transport of gold in hydrothermal ore solutions. *Geochim. Cosmochim. Acta* **37,** 379–399.

Seward T. M. (1991) The hydrothermal geochemistry of gold. In *Gold Metallogeny and Exploration* (ed. R. P. Foster), pp. 37–62. Blackie and Son Ltd., London.

Seward T. M. and Cardile C. M. (1991) Gold adsorption onto colloidal sulphide substrates. In *Source, Transport and Deposition of Metals* (eds. M. Pagel and J. L. Leroy), pp. 707–708. Balkema Press, Rotterdam, the Netherlands.

Seward T. M. and Barnes H. L. (1997) Metal transport by hydrothermal ore fluids. In *Geochemistry of Hydrothermal Ore Deposits* (ed. R. P. Foster), pp. 435–486. John Wiley, New York.

Sha P. (1993) *Geochemistry and genesis of sediment-hosted disseminated gold mineralization at the Gold Quarry mine, Nevada*. Ph.D. dissertation, University of Alabama.

Shenberger D. M. and Barnes H. L. (1989) Solubility of gold in aqueous sulfide solutions from 150 to 350°C. *Geochim. Cosmochim. Acta* **53,** 269–278.

Shirley D. A. (1972) High-resolution X-ray photoemission spectrum of the valence bands of gold. *Phys. Rev. B.* **5,** 4709–4714.

Simon G., Huang H., Penner-Hahn J. E., Kesler S. E., and Kao L. S. (1999a) Oxidation state of gold and arsenic in gold-bearing arsenian pyrite. *Am. Min.* **84,** 1071–1079.

Simon G., Kesler S. E., and Chryssoulis S. L. (1999b) Geochemistry and textures of gold-bearing arsenian pyrite, Twin Creeks Carlin-type gold deposit, Nevada. Implications for gold deposition. *Econ. Geol.* **94,** 405–422.

Sposito G. (1984) *The Surface Chemistry of Soils*. Oxford University Press, New York.

Starling A., Gilligan J. M., Carter A. H. C., Foster R. P., and Saunders

R. A. (1989) High-temperature hydrothermal precipitation of precious metals on the surface of pyrite. *Nature* **340,** 298–300.
Stiller A. H., McCormick B. J., Russel P., and Montano P. A. (1978) Existence and stability of a simple sulfide of iron(III). *J. Am. Chem. Soc.* **100,** 2553–2554.
Stumm W. and Morgan J. J. (1981) *Aquatic Chemistry*. John Wiley, New York.
Sugiura C. (1981) Sulfur K X-ray adsorption spectra of FeS, FeS_2 and Fe_2S_3. *J. Chem. Phys.* **74,** 215–217.
Suleimenov O. M. and Seward T. M. (1997) A spectrophotometric study of hydrogen sulphide ionisation in aqueous solutions to 350°. *Geochim. Cosmochim. Acta* **61,** 5187–5198.
Sun Z., Forsling W., Roenngren L., Sjoeberg S., and Schindler P. W. (1991) Surface reactions in aqueous metal sulfides systems. 3. Ion exchange and acid/base properties of hydrous lead sulfide. *Coll. Surf.* **59,** 243–254.
Sweeney R. E. and Kaplan I. R. (1973) Pyrite framboid formation: Laboratory synthesis and marine sediments. *Econ. Geol.* **68,** 618–634.
Termes S. C., Buckley A. N., and Gillard R. D. (1987) 2p electron-binding energies for the sulfur-atoms in metal polysulfides. *Inorg. Chim. Acta* **126,** 79–82.
Thomas J. E., Jones C. F., Skinner W. M., and Smart R. S. C. (1998) The role of surface sulfur species in the inhibition of pyrrhotite dissolution in acid conditions. *Geochim. Cosmochim. Acta* **62,** 1555–1565.
Tossell J. A. (1996) The speciation of gold in aqueous solution: A theoretical study. *Geochim. Cosmochim. Acta* **60,** 17–29.
Van de Vondel D. F., Van der Kelen G. P., Schmidbaur H., Wolleben A., and Wagner F. E. (1977) Esca study of gold organometallics. *Phys. Scripta* **16,** 367–369.
Vaughan D. J., Becker U., and Wright K. (1997) Sulphide mineral surfaces: Theory and experiment. *Intern. J. Min. Proc.* **51,** 1–14.
Vlassopoulos D. and Wood S. A. (1990) Gold speciation in natural waters: I. Solubility and hydrolysis reactions of gold in aqueous solution. *Geochim. Cosmochim. Acta* **54,** 3–12.
Wächtershäuser G. (1988) Pyrite formation, the first energy source for life: A hypothesis. *System. Appl. Microbiol.* **10,** 207–210.
Wächtershäuser G. (1990) Evolution of first metabolic cycles. *Proc. Natl. Acad. Sci. USA.* **87,** 200–204.
Wei D. and Osseo-Asare K. (1995) Aqueous synthesis of pyrite: Roles of elemental sulfur and Fe(II)/S(II) complexation. V.M. Goldschmidt Conference. 95.
Wertheim G. K. and Buchanan D. N. E. (1977) Core-electron line shapes in X-ray photoemission spectra from semimetals and semiconductors. *Phys. Rev. B.* **16,** 2613–2617.
Widler A. M. and Seward T. M. (1996) Adsorption of gold(I)-hydrosulphide complexes by pyrite. *J. Conf. Abs.* **1,** 699.
Widler A. M. and Seward T. M. (1998) Adsorption of gold(I)-hydrosulphide complexes by iron sulphides. *Mineral. Mag.* **62A,** 1653–1654.
Williams R. and Labib M. E. (1985) Zinc sulphide chemistry: An electrokinetic study. *J. Colloid Interface Sci.* **106,** 252–254.
Wood S. A., Pan P., Zhang Y., and Mucci A. (1994) The solubility of Pt and Pd sulfides and Au in bisulfide solutions: I. Results at 25°-90°C and 1 bar pressure. *Mineral. Deposita* **29,** 309–317.
Yamaguchi S. and Wada H. (1973a) Magnetic iron sulfide of the gamma-Al_2O_3 type. *J. Appl. Phys.* **44,** 1929.
Yamaguchi S. and Wada H. (1973b) Formation de Fe*2S3*. *Bull. Soc. Fr. Min. Crist.* **96,** 213–214.